Downscaling large-scale NCEP CFS to resolve fine-scale seasonal precipitation and extremes for the crop growing seasons over the southeastern United States

**Young-Kwon Lim · Steven Cocke ·
D. W. Shin · Justin T. Schoof ·
Timothy E. LaRow · James J. O'Brien**

Abstract Seasonally predicted precipitation at a resolution of 2.5° was statistically downscaled to a fine spatial scale of ∼20 km over the southeastern United States. The downscaling was conducted for spring and summer, when the fine-scale prediction of precipitation is typically very challenging in this region. We obtained the global model precipitation for downscaling from the National Center for Environmental Prediction/Climate Forecast System (NCEP/CFS) retrospective forecasts. Ten member integration data with time-lagged initial conditions centered on mid- or late February each year were used for downscaling, covering the period from 1987 to 2005. The primary techniques involved in downscaling are Cyclostationary Empirical Orthogonal Function (CSEOF) analysis, multiple regression, and stochastic time series generation. Trained with observations and CFS data, CSEOF and multiple regression facilitated the identification of the statistical relationship between coarse-scale and fine-scale climate variability, leading to improved prediction of climate at a fine resolution. Downscaled precipitation produced seasonal and annual patterns that closely resemble the fine resolution observations. Prediction of long-term variation within two decades was improved by the downscaling in terms of variance, root mean square error, and correlation. Relative to the coarsely resolved unskillful CFS forecasts, the proposed downscaling drove a significant reduction in wet biases, and correlation increased by 0.1–0.5. Categorical predictability of seasonal precipitation and extremes (frequency of heavy rainfall days), measured with the Heidke skill score (HSS), was also improved by the downscaling. For instance, domain averaged HSS for two category predictability by the downscaling are at least 0.20, while the scores by the CFS are near zero and never exceed 0.1. On the other hand, prediction of the frequency of subseasonal dry spells showed limited improvement over half of the Georgia and Alabama region.

Keywords Downscaling · Precipitation · Regional climate · Prediction · Extremes

1 Introduction

Fine-scale seasonal climate prediction has been a very important issue in recent years as near-surface local climate has a considerable effect on many natural systems and human activities. Many studies have therefore developed numerical regional models and statistical models for fine-scale climate prediction over specific geographical areas, including North America (Giorgi 1990; Wilby and Wigley 1997; Wilby et al. 1998; Hong and Leetma 1999; Wilks 1999; Fennessy and Shukla 2000; Widmann et al. 2003; Coulibaly et al. 2005; Salathé 2005; Liang et al. 2006), Europe (Fuentes and Heimann 2000; Huth and Kysely 2000; Huth 2002; Schmidli et al. 2007), Asia (Ji and Vernekar 1997; Kim and Hong 2007), South Africa (Hewitson and Crane 1996), South America (Misra et al. 2003; Robertson et al. 2004; Sun et al. 2006), and Australia (Feddersen and Andersen 2005). The widely accepted basis for regional climate prediction in those studies is to take coarsely resolved information from general circulation

Y.-K. Lim (✉) · S. Cocke · D. W. Shin ·
T. E. LaRow · J. J. O'Brien
Center for Ocean-Atmospheric Prediction Studies (COAPS),
Florida State University, Tallahassee, FL 32306-2840, USA
e-mail: lim@coaps.fsu.edu

J. T. Schoof
Department of Geography and Environmental Resources,
Southern Illinois University, Carbondale, IL 62901, USA

models (GCMs) and downscale the information to local-scale. Downscaling is expected to improve GCM output through enhancement of the spatial resolution. Relative to the GCM, detailed local characteristics of dynamics, physics, and geography can be better incorporated in the downscaling model. Inference of fine-scale climate using direct or interpolated GCM is a questionable practice and may lead to inaccurate regional climate characteristics (von Storch et al. 1993). Therefore, application of downscaling techniques is the most appropriate means of producing fine-scale climate information and providing the best information on local climate.

Many studies have noted that downscaling of precipitation is much more challenging than temperature (Murphy 1999; Schoof and Pryor 2001; Schmidli et al. 2007), because local-scale rainfall by convection is difficult to resolve using only the coarse-scale model simulation. Since this local convection is more vigorous over the low-latitudinal wet region, downscaling over those regions for summer may be even more difficult than other regions and seasons (Murphy 1999; Pandey et al. 2000; Widmann et al. 2003; Feddersen and Andersen 2005). Because of this, many regional precipitation prediction studies over the United States (US) region have focused on the western US (Kim et al. 2000; Leung et al. 2003; Wood et al. 2005; Duffy et al. 2006), where predictive skill is generally higher than the southeastern US, where precipitation is predominantly convective in nature. This study is motivated by the need for regional climate information for crop growing seasons (MAM and JJA) in the southeastern US. This region is a challenging area for successful regional climate simulation but closely linked with natural systems and the human environment, including agriculture, forestry, water management, vegetation, tourism, and urban development.

Fine-scale prediction of precipitation for growing seasons over the southeastern US is urgently needed for several reasons. Local areas within this region frequently experience extremely heavy rainfall and drought. Below or above normal precipitation due to variations in local convection and tropical storms has considerable societal impact. Development of accurate seasonal rainfall prediction tools with high spatial resolution is essential for mitigation of impacts. Also, the southeastern US has large agricultural areas with a variety of products, including peaches, tomatoes, corn, tangerines, peanuts, citrus, strawberries, blueberries, cotton, and dairy. Baigorria et al. (2008) reported that annual variations in yields are highly sensitive to precipitation amounts and the frequency of heavy rainfall and dry spells during these growing seasons. Improved forecasts of seasonal precipitation with high spatial resolution could potentially increase agricultural profits and reduce production risks (Robertson et al. 2007).

Therefore, this study aims to predict the fine-scale seasonal precipitation using a downscaling approach for growing seasons (MAM and JJA) over the southeastern US. This work is also part of ongoing downscaling research performed by Lim et al. (2007), which dealt with surface temperature.

In this study, statistical downscaling will be applied to the National Center for Environmental Prediction/Climate Forecast System (NCEP/CFS) retrospective forecasts at 2.5° resolution (Saha et al. 2006) to produce fine-scale seasonal precipitation. The statistical techniques applied are Cyclostationary EOF (CSEOF) (Kim and North 1997), multiple regression, and time series generation. CSEOF is used instead of conventional eigentechniques, such as regular EOF and Canonical Correlation Analysis (CCA), because CSEOF is very useful in extracting the complete spatio-temporal evolution of the significant climate signals (e.g., the seasonal cycle, prominent intraseasonal oscillations, and ENSO-related evolution) over a cyclic period (Kim and Wu 1999). We expect that data decomposition in this way enables the subsequent regression method to better extract the NCEP/CFS evolution patterns physically consistent with evolutions of the observational climate signals. CSEOF and multiple regression are trained with lower mode Principal Components (PCs) of the observations and the NCEP/CFS to determine their statistical relationship. This regression approach is consistent with Widmann et al. (2003) in that the numerical global model precipitation is used as a predictor. Their study reported improved predictive skill over conventional approaches, which obtain large-scale predictors from other variables.

Once the large-scale evolution patterns associated with the fine-scale observational climate signals are found, we need to generate the PC time series for the prediction period. While conventional PC time series often exhibit high-frequency fluctuations, the CSEOF PCs vary slowly with time. Lim and Kim (2006) found that this characteristic facilitates the generation of the PC time series for the prediction period more reliably. As a result, improved localized climate information from coarsely resolved model forecasts is expected. Using the fine-scale climate forecasts, our study will discuss the current quality of downscaled spring and summer precipitation over the southeastern US. We expect this study to contribute substantially to the improvement of fine-scale climate prediction for the southeastern US, since few studies have critically attempted to downscale spring and summer precipitation for this region.

The remainder of this paper is organized as follows. The NCEP/CFS data and the observational data are described in Sect. 2. Downscaling methods including experimental design are addressed in Sect. 3. Section 4 describes the

downscaled precipitation and its predictive skill, followed by concluding remarks and discussion in Sect. 5.

2 The CFS model data and observation

2.1 The NCEP/CFS retrospective forecasts

The CFS, the fully coupled model representing the interaction between oceans, land and atmosphere, was developed for the purpose of dynamical seasonal prediction at the Environmental Modeling Center (EMC) at NCEP. The CFS provides daily atmospheric variables at 2.5° lat/lon resolution from the retrospective forecasts. Seasonal integrations initialized in each calendar month of the year simulate global atmospheric fields out to 9 months into the future, covering a period of 26 years from 1981 to 2006. In this study, we used ten member integration data (March through August each year) with lagged initial conditions centered in February. The initial dates from the last date of February, in descending order, are 28, 27, 23, 22, 21, 20, 19, 13, 12, and 11. These initial dates are based on the pentad ocean initial condition in the CFS (Saha et al. 2006). The period used for downscaling was, however, limited to 19 years from 1987 to 2005 because the gridded observation data verified by the Florida Climate Center was available for this 19-year period. Since these observational data are used for statistical training with the CFS data, the temporal lengths of these two data sets need to be identical. The atmospheric initial conditions of the CFS were given from the NCEP/DOE Atmospheric Model Inercomparison Project (AMIP) II Reanalysis (Kanamitsu et al. 2002) and the ocean initial conditions were given from the NCEP Global Ocean Data Assimilation (GODAS). The atmospheric component of the CFS is a lower-resolution version of the Global Forecast System that was the operational weather prediction model at NCEP. The ocean component is the GFDL Modular Ocean Model version 3. For the land surface hydrology, the two-layer model described in Mahrt and Pan (1984) was used. More details on the CFS reforecasts are found in Saha et al. (2006).

2.2 Observed precipitation

The origin of the observed precipitation in this study is the National Weather Service (NWS) Cooperative Observer Program (COOP). The COOP has more than 100 years of observational data which help define the climate of the US and measure long-term climate change. COOP weather stations are densely distributed over the entire US territory and record daily weather observations (http://www.nws.noaa.gov/climate/). The gridded dataset for the southeastern US region was provided by the Florida Climate Center

(http://www.coaps.fsu.edu/climate_center/). The data period in this study covers the period of 1987 to 2005 with a daily time interval.

The original station data (Fig. 1 lower panel) were converted to 20 km × 20 km grids using the Cressman objective analysis (OA) scheme (Cressman 1959). As a result, each county has one grid point on average in Georgia, where the area of each county is relatively smaller than in other states. Florida and Alabama have one or two local grid points in most counties. The conceptual basis of this OA scheme is the same as the method described in Sect. 3.2. The gridded dataset has 1,252 grid points with 20 km resolution, covering Florida, Georgia, and Alabama. Gridded spatial fields are compared with those from the station data and we confirmed that the fields are nearly consistent.

3 Methodology

3.1 Statistical downscaling model

Statistical downscaling encompasses a large number of methods, ranging in complexity from simple interpolation to eigentechniques, regression methods, stochastic time series models, and artificial neural networks (Trigo and Palutikof 2001; Reusch and Alley 2002; Ramírez et al. 2006). The statistical downscaling framework in this study comprises Cyclostationary EOF (CSEOF) technique (Kim and North 1997), multiple regression, and the time series generation. As briefly introduced in Sect. 1, CSEOF (Kim and North 1997) is an analysis technique for extracting the spatio-temporal evolution of the significant climate signals (e.g., seasonal cycle, ENSO, and dominant intraseasonal oscillations, etc.), which we call physical modes, and their seasonal to interannual amplitude variations. CSEOF analysis is conducted on the basis of a cyclostationary process in which the statistical properties vary cyclically with time. Thus, space-time data (P) in CSEOF analysis are represented as:

$$P^o(r^o, t) = \sum_n S_n^o(t) B_n^o(r^o, t) \qquad (1)$$

$$P^g(r^g, t) = \sum_n S_n^g(t) B_n^g(r^g, t) \qquad (2)$$

where $B_n^o(r^o, t)$ and $B_n^g(r^g, t)$ are time-dependent cyclostationary eigenfunctions from observation and large-scale CFS, respectively. $S_n^o(t)$ and $S_n^g(t)$ are their principal component (PC) time series. Parameters, superscripts, and subscripts here represent o: observation, g: global, n: mode number, r: spatial grid point, and t: time. The purpose of applying CSEOF analysis is to extract the spatio-temporal evolution of prominent climate signals and their amplitude
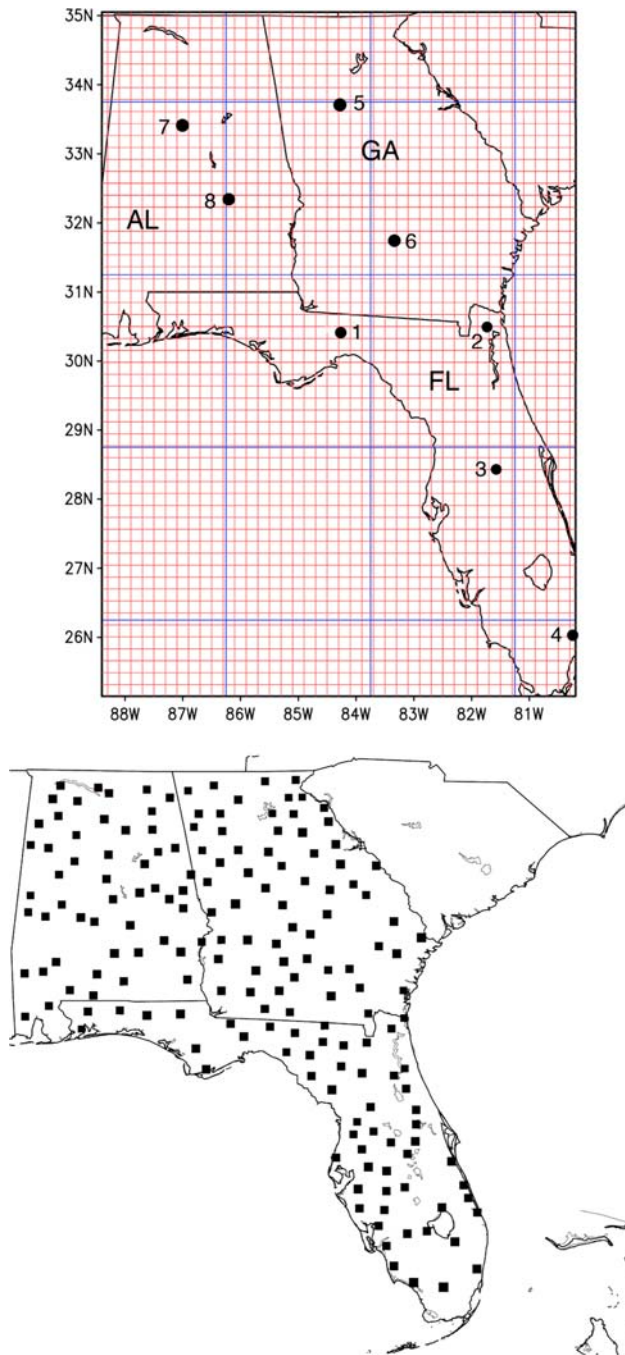
Fig. 1 *Upper* Geographical areas of three states (FL Florida, GA Georgia, AL Alabama) in the southeastern United States where the CFS precipitation is localized by downscaling methods. *Blue lines* over the domain represent the spatial grid cells of the CFS whereas *red lines* represent the local grid points applied in the statistical downscaling model. *Eight dots with numbers* represent locations of cities, *1* Tallahassee, *2* Jacksonville, *3* Orlando, *4* Miami, *5* Atlanta, *6* Tifton, *7* Birmingham, and *8* Montgomery. *Lower* A map showing the station locations used for gridded observation data

variations from the observation and the CFS data, respectively. Therefore, CSEOF analysis, as the first step of this downscaling, was applied to the daily observation and the

CFS data, respectively, for the 18-year training period (March through August each year). The remaining year was regarded as the prediction period during which we perform the fine-scale prediction. Therefore, application of CSEOF for the training period was carried out a total of 19 times by leaving out each of the years from 1987 to 2005 in turn under a cross-validation basis. The spatial domain for applying CSEOF to the CFS data is 90°W–75°W and 25°N–40°N, which is large enough to recognize the large-scale characteristic patterns encompassing the southeastern US.

The next step is to use multiple regression to find the statistical relationship between the prominent climate signals of the observations and the CFS. Multiple regression was applied to the extracted climate signals and the corresponding PC time series obtained from both observation and the CFS. To find the regressed evolution patterns, the observed CSEOF mode was declared as a target (predictand) followed by regression of the CFS CSEOF mode (predictor) onto the target. For this regression, the PC time series of the first ten modes of a predictor, which explain approximately 70% of the total precipitation variance, were regressed onto a particular PC time series of the target (observed CSEOF PC) by multiple regression. This indicates that we use the modeled precipitation as a predictor, similar to an approach addressed in Widmann et al. (2003). Variance by the first ten modes contributes substantially to the overall variance. The remaining several tens of modes accounted individually for a smaller fraction of total variability and contributed relatively little to overall predictability. Therefore,

$$S_n^o(t) = \sum_{i=1}^{10} \alpha_{ni} S_i^g(t) + \varepsilon(t), \qquad i = 1, 2, \ldots, 9, 10 \qquad (3)$$

where $S_n^o(t)$ are the nth mode target PC time series, α_{ni} are the regression coefficients, and $S_i^g(t)$ are the predictor PC time series. Regression coefficients were determined such that the variance of regression error, $\varepsilon(t)$, is minimized. Once regression coefficients were computed, they were weighted for each mode ($i = 1, \ldots, 10$) of predictor eigenfunctions to construct the regressed large-scale CFS patterns ($\mathrm{Breg}_n^g(r^g, t) = \sum_i \alpha_{ni} B_i^g(r^g, t)$), which we assume are physically consistent with the nth mode of predictand eigenfunctions. Figure 2 is the example representing the 1st CSEOF modal patterns from observation ($B_1^o(r^o, t)$) (left two columns) and the regressed CSEOF patterns of the CFS ($\mathrm{Breg}_1^g(r^g, t)$) (right two columns) onto the 1st observational mode via multiple regression. Since CSEOF was applied to the daily data, CSEOF modes were produced at daily time steps. In Fig. 2, we took the temporal average of the 1st CSEOF modal patterns over ∼30 days and showed them for each season (MAM and JJA). Spatial
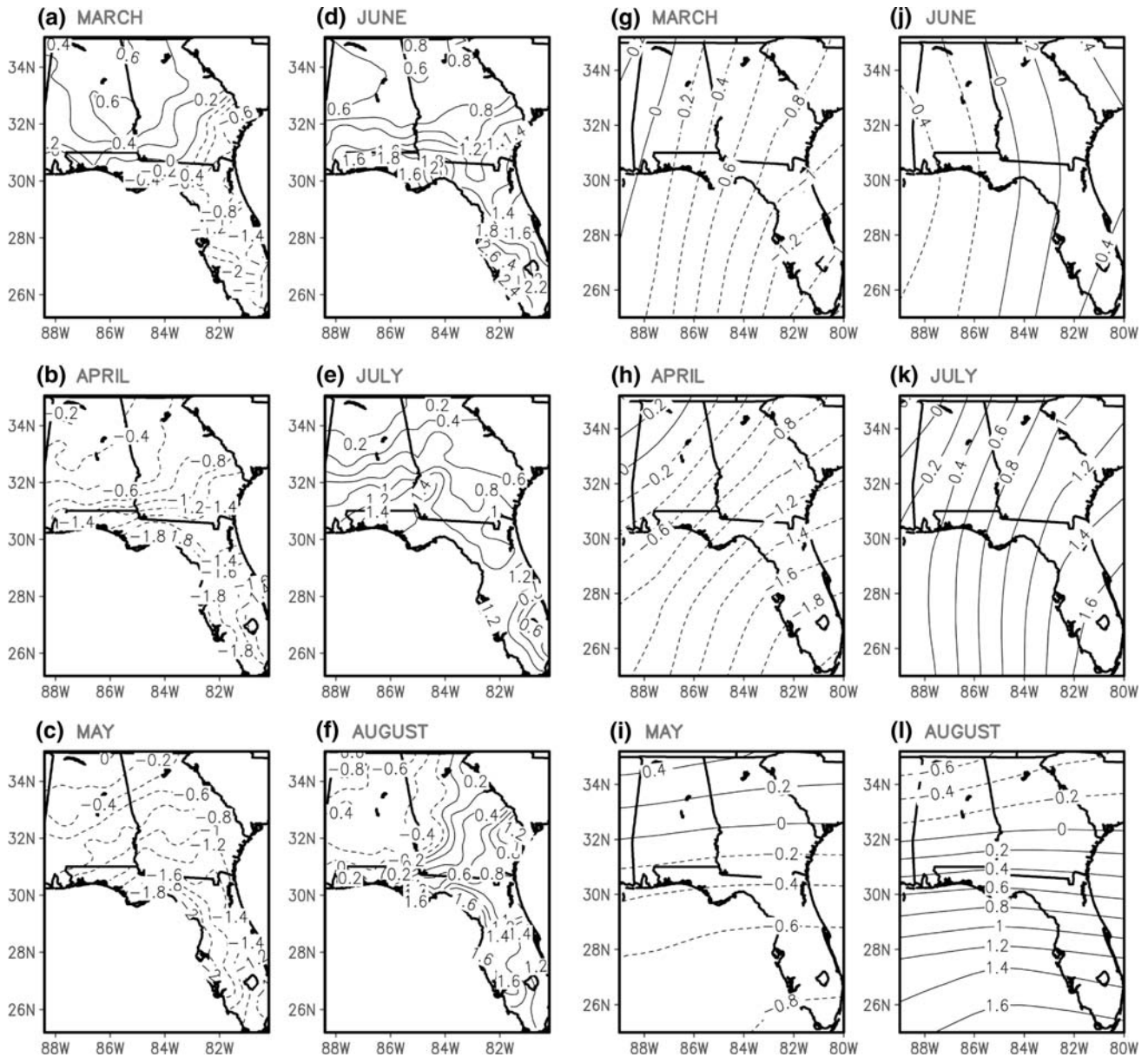
Fig. 2 *Left two columns* (**a–f**) The 1st mode CSEOF patterns for observation. *Right two columns* (**g–l**) CSEOF patterns for the GSM, which are obtained by regression onto the first observed CSEOF mode. CSEOF patterns originally at daily time step have been averaged over each month to produce the maps shown

patterns show how certain biased CFS anomalies have been regressed onto the observed 1st CSEOF patterns. On the basis of this relationship, the downscaling procedure can correct biases contained in the CFS data.

Based on the statistical relationship between the observed climate signals and the CFS data identified from 18-year training, CSEOF PC time series were generated for the prediction period (the remaining year) (Fig. 3). The equation for the PC time series generation is given as

$$S_n^g(t_p) = P^g(r^g, t_p) \cdot \text{Breg}_n^g(r^g, t), \qquad (4)$$

where $S_n^g(t_p)$ are the generated nth mode PC time series, $\text{Breg}_n^g(r^g, t)$ are the regressed eigenfunctions of the CFS for the nth mode obtained from training, r^g is the CFS grid point, and $P^g(r^g, t_p)$ are the CFS anomalies in the prediction period. The anomaly value is the departure from the mean over the training period.

The downscaled data were constructed using the generated PC time series and observed eigenfunctions identified from training (Fig. 3). This is the process of fitting the CFS anomalies represented by PC to the observed statistics only

Fig. 3 Schematic diagram of downscaling procedure in the present study. Downscaling has been conducted using Cyclostationary EOF, multiple regression, and the time series generation techniques. Downscaled data are produced over 19 years (1987–2005) under the cross-validation framework
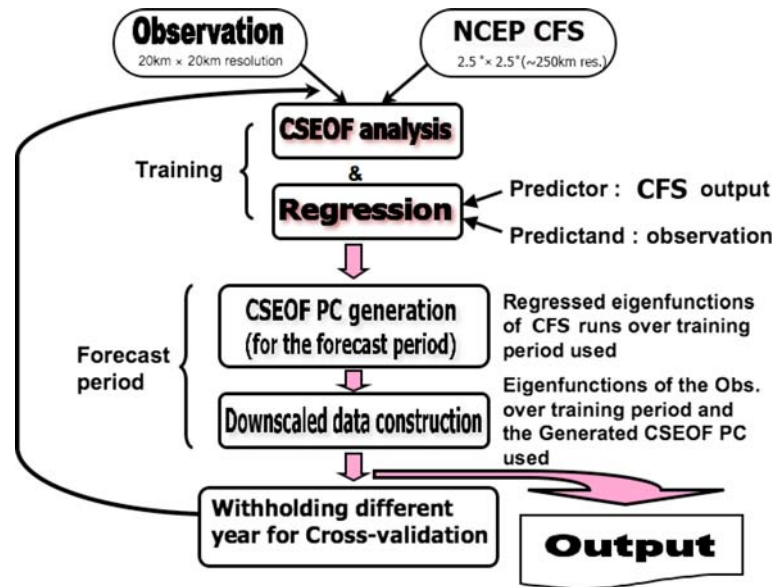
for the training period. The downscaled data were finally constructed by

$$D(r^o, t_p) = \sum_n S_n^g(t_p) \cdot B_n^o(r^o, t), \qquad (5)$$

where $S_n^g(t_p)$ are the generated PCs obtained from Eq. 4, $B_n^o(r^o, t)$ are the CSEOF eigenfunctions of the observation for the training period (Eq. 1), and $D(r^o, t_p)$ is the downscaled precipitation at local grid point r^o over the prediction period t_p.

The downscaling procedure delineated in this section was repeated under cross-validation by leaving out each year from 1987 to 2005. The remaining 18 years were used to develop a downscaling model for prediction of the omitted year. As a result, downscaled daily precipitation for the entire 19 years has been constructed. The overall downscaling procedure is illustrated by the flow chart in Fig. 3.

3.2 Localization of the CFS data via objective analysis and bias correction

OA in conjunction with bias correction was applied to each member of CFS data as a simple localization. This was conducted for comparison with downscaled precipitation and its frequency of extremes in terms of categorical predictability. For the OA of the CFS precipitation, we applied the Cressman OA scheme (Cressman 1959), which makes successive corrections to an initial guess. Therefore, multiple steps were made through the grid with increasingly smaller radii of influence. At each step, the correction factor based on a distance weighted formula was applied to errors in order to minimize them. An error is defined as the difference between the value at the CFS grid point and the interpolated value at the fine-scale grid point.

Once OA was completed, bias correction was applied to this interpolated CFS data. The conceptual basis of this bias correction is equivalent to that described in Wood et al. (2002). This method consists of remapping the exceedence probabilities (percentiles) of the objectively analyzed CFS data to those of the observed data so that both datasets have identical climatological mean and probability distribution. Schoof et al. (2009) found that this bias correction is also useful for removing the systematic error of the model data.

The basic rationale for the method is that we replace the OA outputs with values that have the same percentiles as those seen in observations. For example, if an OA value of precipitation lies at the 70th percentile of the OA precipitation distribution (that is, not to be exceeded more than 30% of the time), the bias-corrected value would be the 70th percentile of the observed precipitation distribution. For this bias-correction, we estimated the probability distribution for each month at each grid cell (20 km × 20 km) using daily OA values and observations, respectively. From the percentile value of the OA precipitation, we calculated the associated value having the same exceedence probability in the observed probability distribution in order to switch the OA value to the associated value. We repeated the above correction for each month such that it is treated independently and seasonal variations in bias can be considered.

3.3 Categorical predictability evaluation by Heidke Skill Score

Categorical predictability of the seasonal precipitation anomalies and the subseasonal extreme events (e.g., frequency of heavy rainfall days and subseasonal dry spells)

was assessed at individual grid points in terms of the Heidke skill score (HSS) (Heidke 1926; Jolliffe and Stephenson 2003). The HSS is a commonly used categorical verification score which measures categorical matches between forecasts and observations (Barnston 1992). Two category (above/below climatological average), and three category (above/near/below average) classification methods have been considered, respectively, for HSS calculation in this study. The threshold values for three category classification are ±0.5 standard deviation, or ±1 standard deviation from the climatological mean. Based on the HSS formula (Heidke 1926), positive and negative HSS values indicate, respectively, skill above and below that of random chance.

3.4 Definition of heavy rainfall days and dry spell

In order to evaluate the performance of the downscaling in producing the interannual variation of the frequency of subseasonal extreme events, we investigated the frequency (MAMJJA) of heavy rainfall days and subseasonal dry spells each year. We counted the frequency of those events each year in each member run and averaged the resulting frequencies over ten members. Then we compared the performances between downscaling and the objectively analyzed CFS with bias correction.

A heavy rainfall day is defined as a rainy day with the rainfall amount exceeding the certain standard deviation value (e.g., 0.5, 1, and 2) above observational daily climatology. A dry spell is a period of precipitation below a specific amount. The specific period and amount of precipitation used for the definition of a dry spell can vary depending on the particular consideration. In this study, a dry spell is defined as a 1 week period (or 10 day period) with the accumulated rainfall less than 0.1 mm/day (Robertson et al. 2004).

4 Results

### 4.1 Downscaled fields and long-term variation

The daily CFS precipitation to be downscaled in this study has been summed for each season and the resulting seasonal patterns are shown in the top panel of Fig. 4 [mm] for a preliminary comparison with the observed data. In this figure, the seasonal precipitation amount for each year has been averaged over 19 years. Observations are shown on the middle panel. Observation data originally at 20 km resolution were objectively analyzed to the CFS grid resolution (2.5 lon.-lat. degree) using the Cressman OA scheme (Cressman 1959). The observed field shows that more precipitation is found in the continental area than the

southern coastal region (e.g., Florida) in MAM (Fig. 4b), whereas the reversed characteristic feature is found in JJA (Fig. 4e). This feature is reasonably reproduced by the CFS to a certain extent. However, the CFS data over most grid points exhibit overestimation, which could be associated with positive biases of the CFS precipitation on wet days (Higgins et al. 2008). Exceptions are found over the northwestern tip of Florida and southwestern Alabama (Fig. 4a, b, d, e). Overestimation is more distinct over Georgia, resulting in a precipitation amount comparable to Florida in JJA (Fig. 4d). The observed precipitation over Georgia is less than Florida, where the precipitation amount reaches the maximum (Fig. 4e). Overestimation by the CFS in MAM is also prominent in Georgia. The precipitation amount in Georgia is comparable to that over Alabama (Fig. 4a), where more observed precipitation is recorded than Georgia (Fig. 4b). Additionally, in the CFS precipitation, the eastern domain tends to have more precipitation than the western domain. Observed fields, however, do not exhibit these east-west differences in either season.

The CFS skills in the southeast US were reported as very low in previous studies (Saha et al. 2006). Particularly, the CFS precipitation for spring and summer has been much harder to predict than for winter. As shown in the bottom panel of Fig. 4, the majority of grid points exhibit near zero correlations (−0.1–0.2) between observation and the CFS summer precipitation (Fig. 4f). The correlations are relatively higher in spring but they lie in the 0.0–0.3 range (Fig. 4c).

Approximately 150 local-scale grid cells have been created within the single CFS grid cell as a result of downscaling (Fig. 1a), and the downscaled data produce fine-scale distribution of precipitation with significant reduction in biases (Figs. 5, 6). The capability of the downscaling to reproduce both long-term and short-term precipitation characteristics was investigated. First, in order to investigate the reproduction of long-term (~5 years) variation as shown by the running averaged time series in Fig. 7a (green solid), downscaled daily precipitation was summed over 6 months (MAMJJA) each year at individual grid points. Then, the accumulated precipitations for each year were averaged for the period of 1987–1990 and the following 5 years (1991–1995), respectively; resulting distributions are shown in Fig. 5. Additional 5 year mean distributions for the remaining period (e.g., 1996–2000 and 2001–2005) are presented in Fig. 6. Figures 5 and 6 illustrate the capability of this downscaling model in producing fine-scale climate information on an interannual time scale from the coarsely resolved model data. Downscaled fields were plotted in the middle panel, along with their comparison with observations (bottom panel) and CFS data (top panel). Figure 5

Fig. 4 *Left column* Ensemble averaged 19-year seasonally accumulated precipitation [mm] for MAM. *Figures from the top row* represent the distribution of precipitation from the CFS, objectively analyzed observation to the CFS grid scale, and correlations between them. The scale is denoted by *color bar* attached on the right side. *Right column* Same as the left column but for JJA season
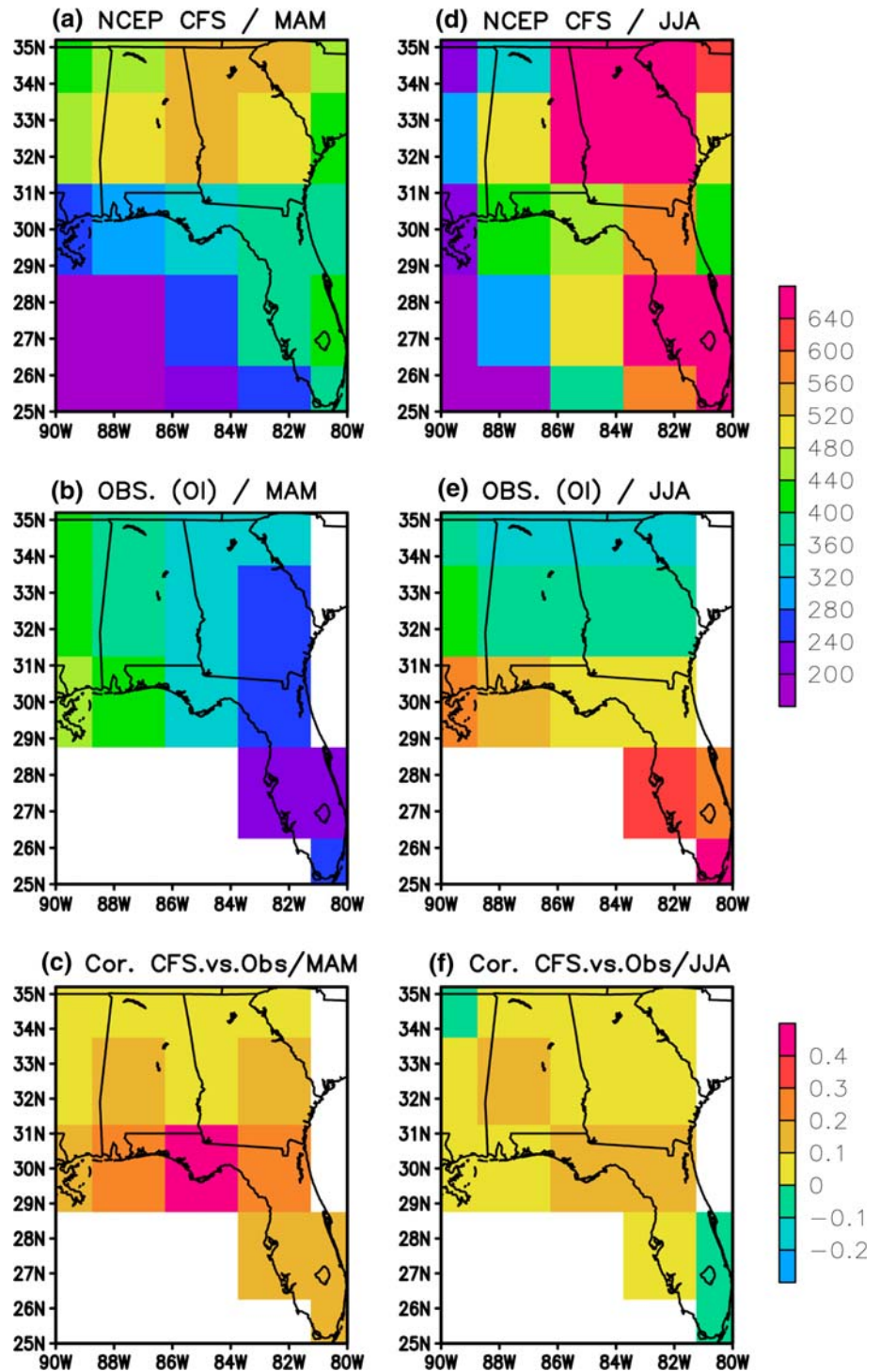
reveals that observed rainfall change between two periods is reasonably reproduced by the downscaling. Also, the regional distribution of the downscaled field is quite consistent with the observed field (Fig. 5b, c, e, f). Precipitation maxima over the Florida panhandle and southwestern Alabama, and minima over central Georgia, were accurately captured by the downscaled fields. In addition, wet

biases unveiled from the CFS have been significantly reduced by the downscaling. The coarse-scale CFS spatial features on the top panel are apparently different from observed mean patterns. As seen in Fig. 5a and d, the CFS spatial fields only describe the coarse-scale patterns. Wet biases are found all over the domain although precipitation change between the two periods is properly distinguished.

Fig. 5 *Left column* Ensemble averaged precipitation [mm/ MAMJJA] field for the period of 1987–1990. *Figures from the top row* represent the distribution of precipitation from the CFS, downscaling, and observation. The scale is denoted by *color bar* attached on the right side. *Right column* Same as the left column but for the period of following 5 years (i.e., 1991–1995)
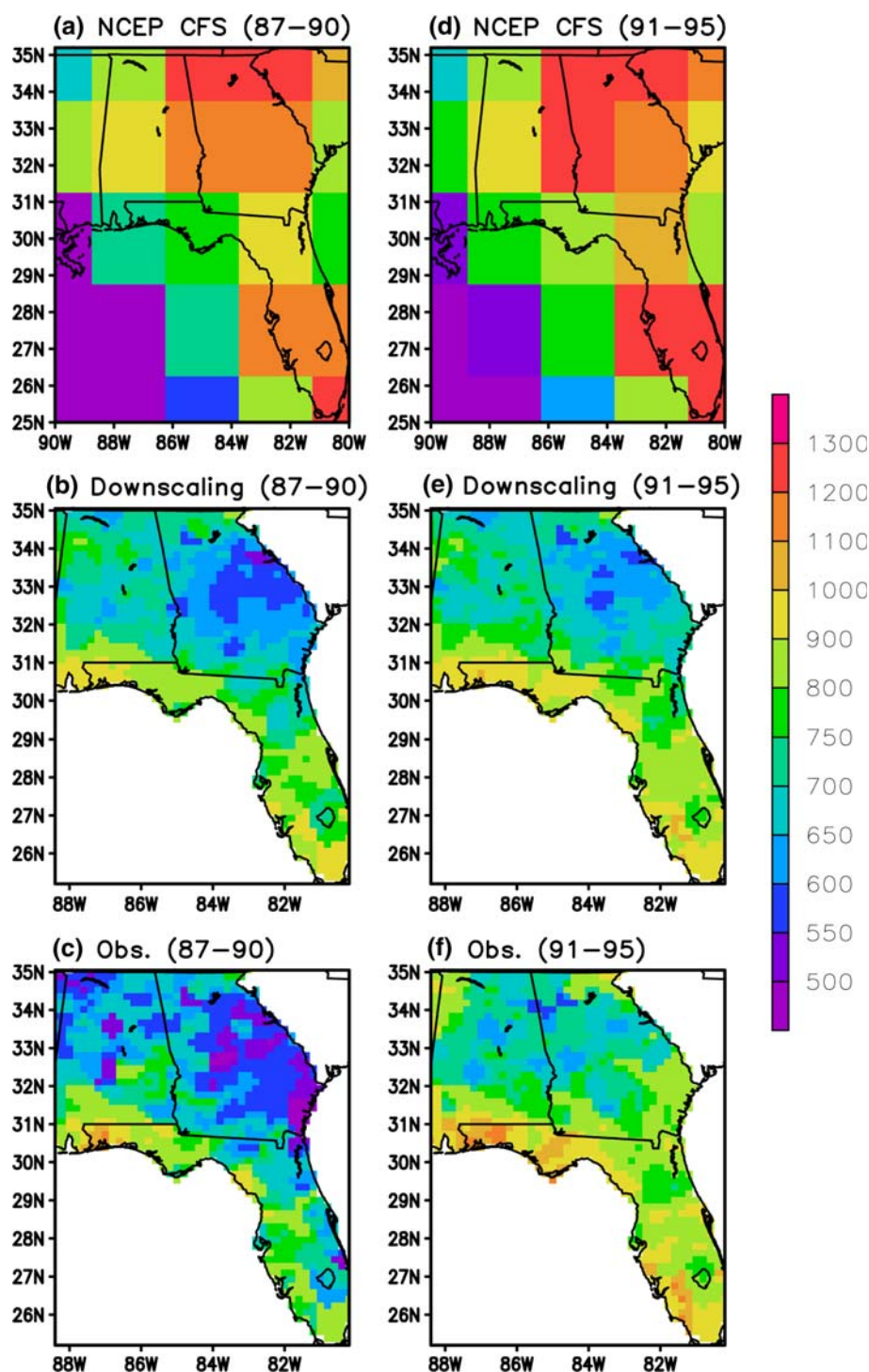
These spatial features of Fig. 5 are found again in Fig. 6. Reduction in bias, precipitation variation, and detailed local patterns were faithfully realized through the application of the downscaling technique. Consequently, the downscaled 5 year means reasonably reproduced the observed rainfall oscillation with long-term cycles (Figs. 5c, f, 6c, f), which is a feature reported for the US region (Groisman and Legates 1994).

Figure 7a again compares the observation (black bar) with downscaled data (red) and CFS data (blue), respectively, in terms of their annual (MAMJJA) rainfall each year for the entire 19 years. In this figure, we took the area average over the whole domain and then plotted the annual precipitation (Fig. 7a). The CFS rainfall tends to overestimate the observed precipitation, confirming the wet biases described in the previous paragraph. In addition, the

Fig. 6 Same as Fig. 5 but for the period of 1996–2000 (*left column*) and the period of 2001–2005 (*right column*)
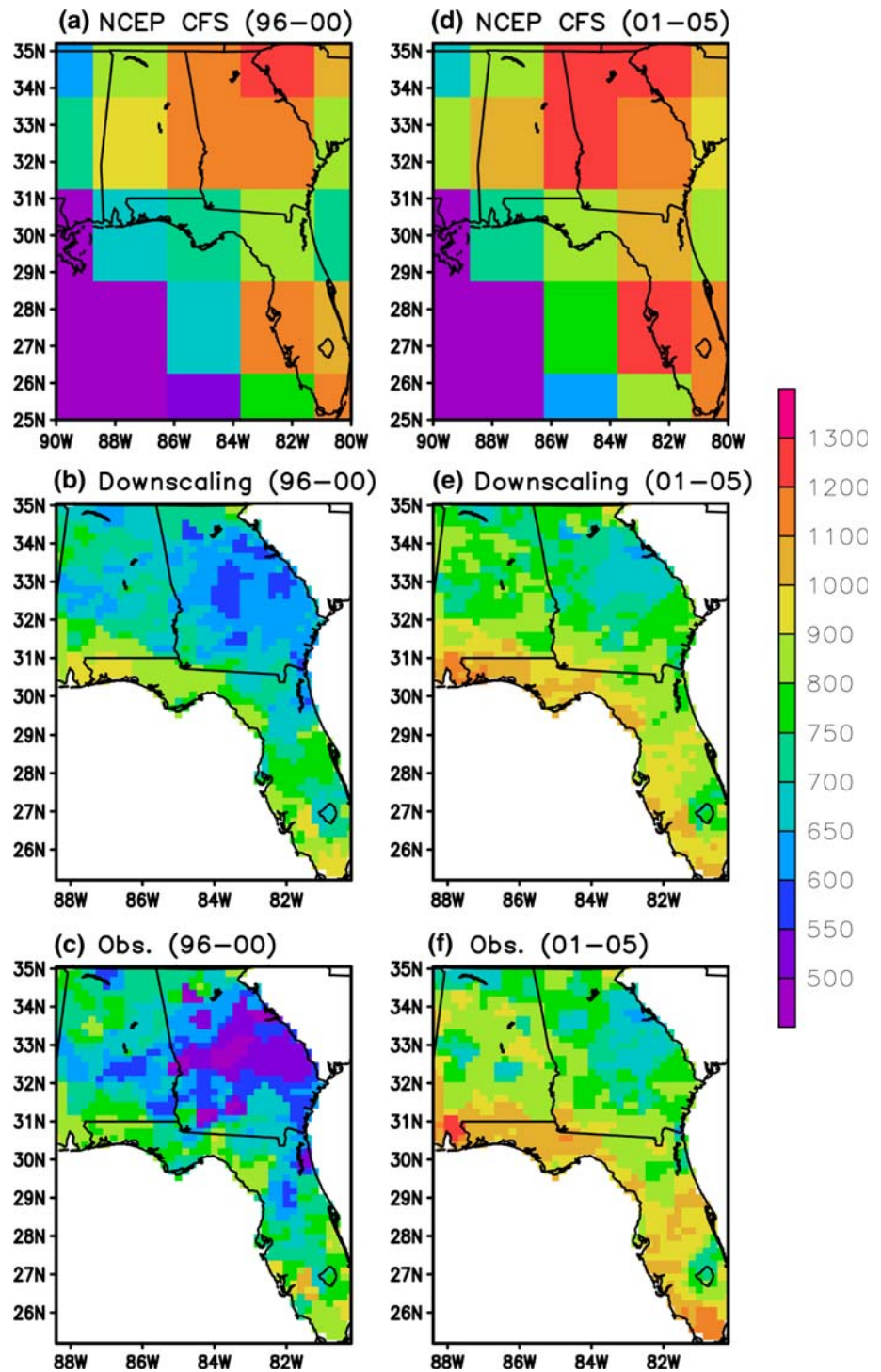

interannual change in rainfall amount (i.e., temporal variance) is smaller than that of downscaled rainfall (standard deviation ratio (Down./Obs.) = 0.70, (CFS/Obs.) = 0.40). The root mean square error (RMSE) of the CFS data is substantially reduced by downscaling (RMSE (Down.) = 145 mm, RMSE (CFS) = 207 mm). Correlations of the observational rainfall with the two modeled data sets

(downscaling and CFS) are, respectively, 0.41 and 0.11, indicating that the downscaling outperforms the CFS forecast. This correlation by downscaling is statistically significant at 90% confidence.

It appears that Fig. 7a does not reflect any persistent correlations with ENSO, as the weak relationship in summer was discussed in previous studies (e.g., Hu and Feng

Fig. 7 Year-to-year variation of the ensemble averaged precipitation [mm] summed over each year (MAMJJA) (*top panel*), MAM (*middle panel*), and JJA (*bottom panel*) obtained from the observation (*black bars*), downscaling (*red bars*), and CFS (*blue bars*). Precipitation at each grid point is area-averaged over the whole southeastern US domain. Ratio of the standard deviation to the observational standard deviation, root mean square error, and correlation with the observation are provided in the upper corner of each panel. The *green solid time series on the top panel* represent the running averaged (±2 years) observational precipitation plotted by *black bars*
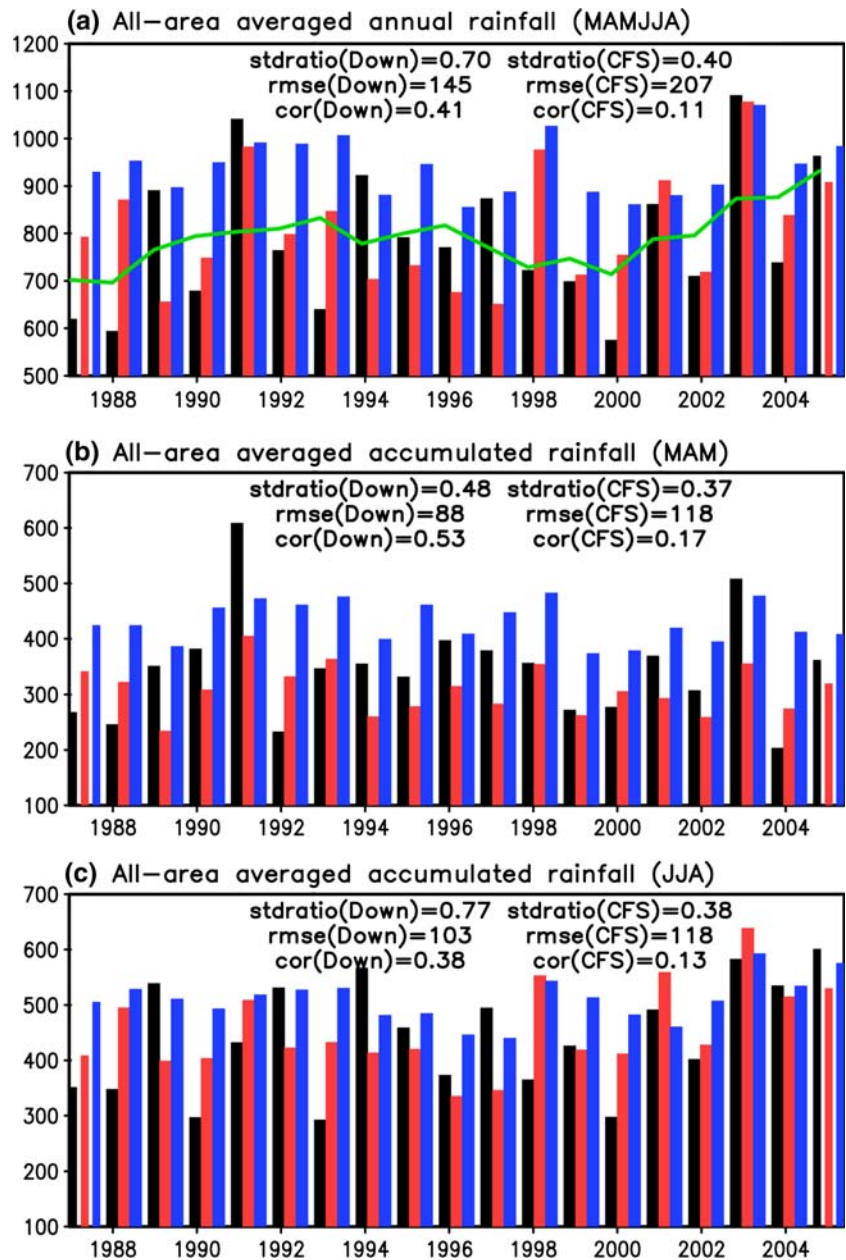
2001). As noted in Gershunov et al. (2003), unclear linkage with ENSO seems an unfavorable condition for achieving great seasonal predictability in this region.

4.2 Seasonal precipitation

Downscaling also improves the forecasts of precipitation at the seasonal timescale. Area-averaged seasonal rainfall for spring (MAM) and summer (JJA) are shown in Fig. 7b and c, respectively. At the seasonal timescale, CFS precipitation exhibits overestimation and overdispersion (under-estimation of variance) and larger RMSE than the downscaled precipitation (see the corresponding values in each panel). Correlation values have been substantially increased by ∼0.3 (MAM from 0.17 to 0.53, JJA from 0.13 to 0.38) through downscaling. Correlations achieved by downscaling are statistically significant at 95% confidence for MAM but not significant for JJA. Since the CFS precipitation utilized for this downscaling is not skillful and summer precipitation is relatively hard to predict, the increase of ∼0.25 is lower than the significance threshold at 95% confidence.

We examine the year-to-year variation of this seasonal total precipitation at individual local grid points. The downscaled seasonal rainfall [mm] were plotted for the eight selected grid points representing four cities in Florida (Tallahassee, Orlando, Jacksonville, and Miami), two cities in Georgia (Atlanta and Tifton) and two cities in Alabama
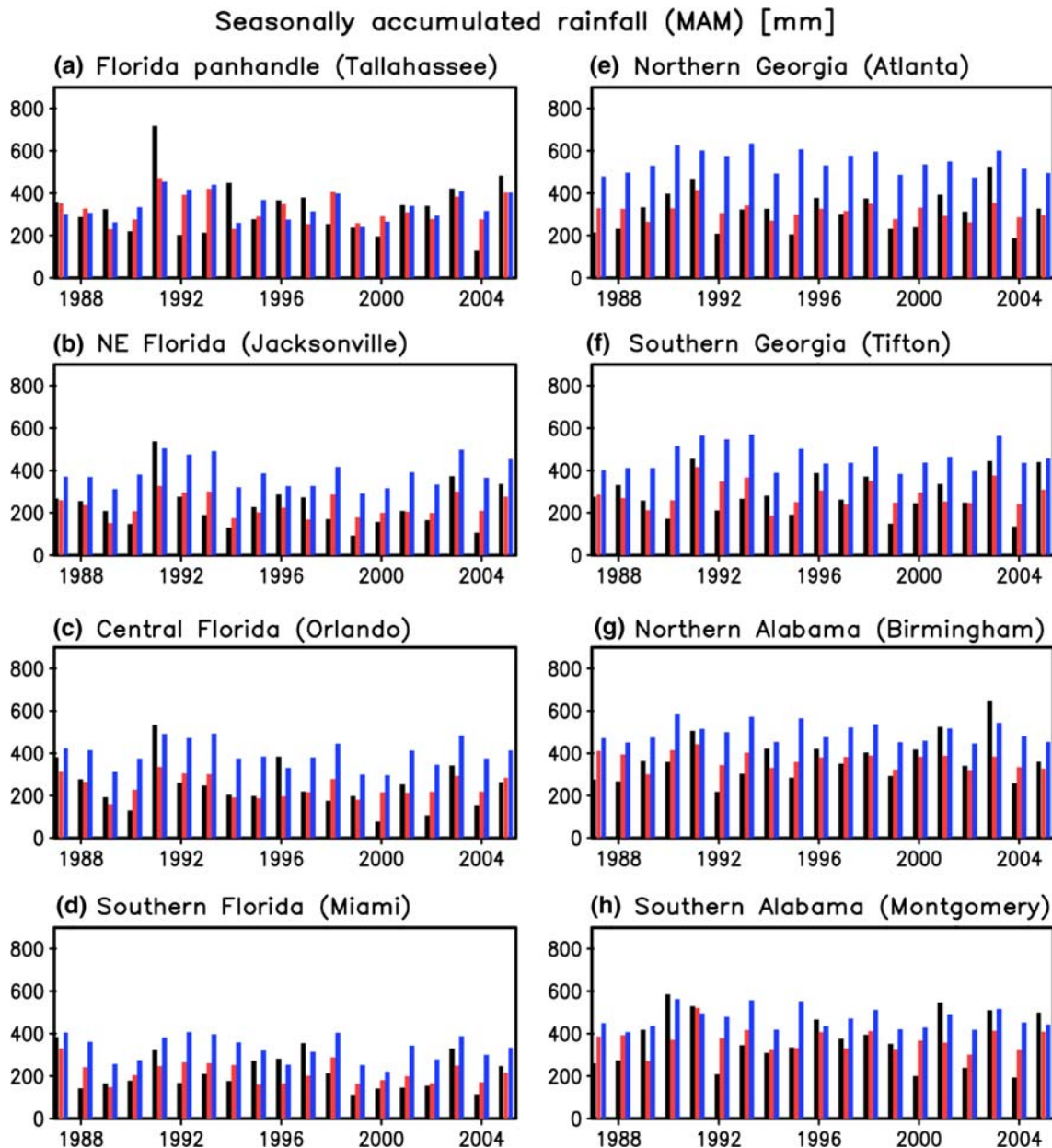
Seasonally accumulated rainfall (MAM) [mm]

Fig. 8 Year-to-year variation of the ensemble averaged seasonal precipitation. Daily precipitation has been summed over MAM [mm] each year for the selected local grid points. Precipitation from observation, downscaling, and CFS is, respectively, denoted by *black,*

red, and blue bars. Downscaled daily precipitations are summed over MAM each year for each ensemble member, followed by taking the average over ensemble members. The same averaging has been applied to observation and CFS, respectively, for comparison

(Birmingham and Montgomery). The grid points were selected to provide an evenly distributed representation of the southeastern US domain (see Fig. 1a). Each city also represents a specific subregion of the southeastern US: the Florida Panhandle, NE Florida, C. Florida, S. Florida, N. Georgia, S. Georgia, N. Alabama, and S. Alabama. Figs. 8 and 9 show the seasonal rainfall over those cities, respectively, for spring (MAM) and summer (JJA). The CFS values with 20 km resolution were constructed for

comparison with the downscaling. They were obtained by assuming that the CFS values are the same at all local grid points within the CFS grid, which in turn indicates that a given CFS value at a local grid point is equivalent to a value at the nearest CFS grid (Murphy 1999). As seen in Fig. 8 and 9, overall features at a glance indicate that observed variations (black bars) are reasonably captured by downscaled data (red). The CFS data (blue bar) tend to overestimate the observed time series (e.g., Figs. 8b–h,
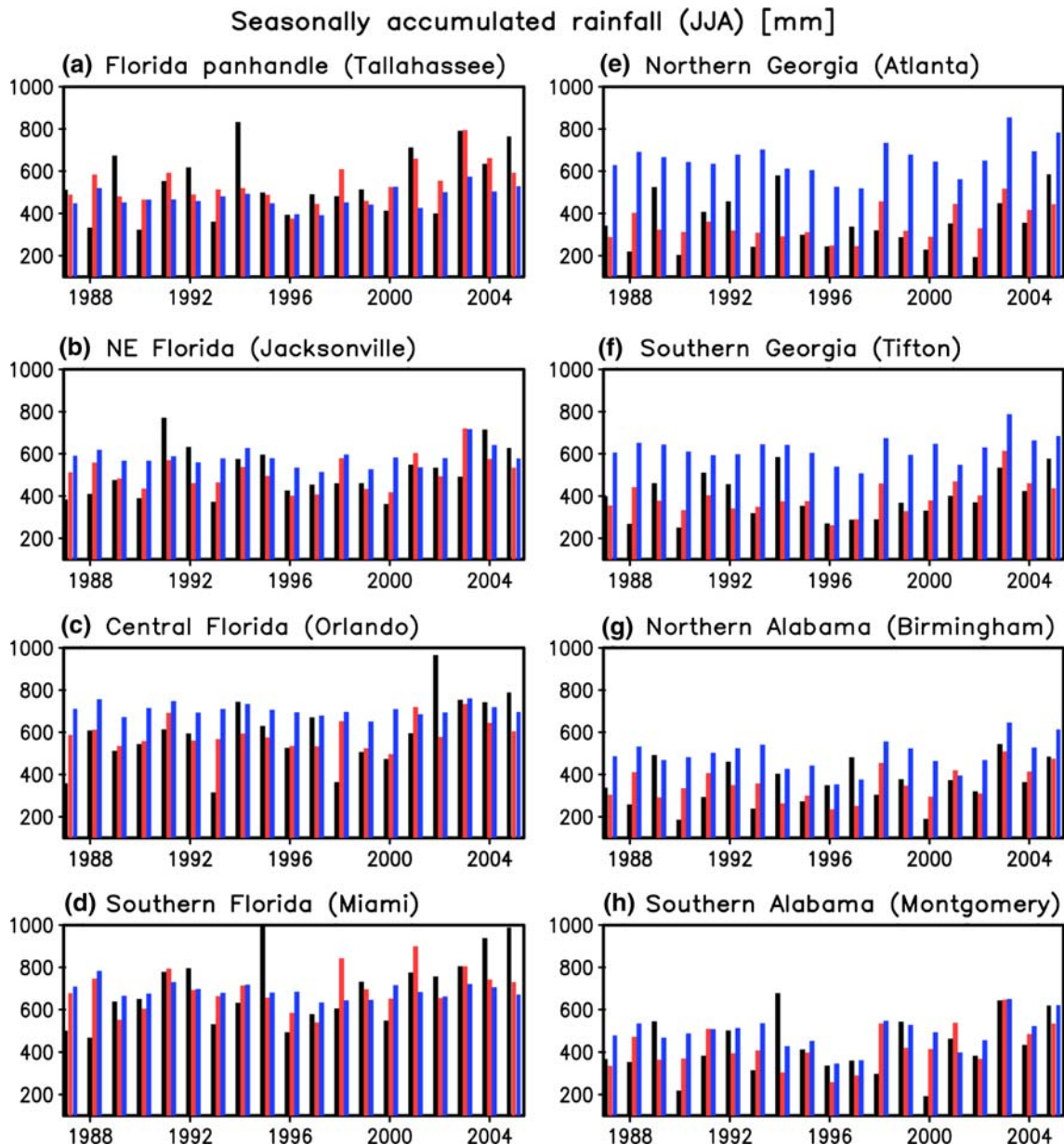
Fig. 9 Same as Fig. 8 but for JJA

9e–g). Predictability by downscaling appears greater since 1999, with less agreement in the early period (e.g., 1988, 1989, and 1994). Poor capture of the observed peaks appeared in the 1994 JJA (Fig. 9a, e, f, h), and the largest error produced within the downscaled data was in the 1995 JJA in Miami (Fig. 9d). Nonetheless, overall features indicate the noticeable increase in correlation and reduction in RMSE by downscaling at all cities (Table 1). In particular, the CFS forecasts for summer precipitation show smoothed year-to-year variation with much smaller amplitude than that of observation (see standard deviation ratio). The correlation skill of the downscaled data is relatively higher than that of the CFS data. Improvement of the correlation values shows wide variation between local stations. For instance, Tallahassee shows correlation improved by 0.1 while Atlanta shows correlation increase by 0.49. Correlations over six cities (Jacksonville, Orlando, Miami, Atlanta, Tifton, and Montgomery) exceed statistical significance threshold at 90% confidence. Again, since the present downscaling attempts the skill improvement from the nearly unskillful coarse-scale data, the number of cities where the correlation satisfies the significance at 90% confidence for summer is reduced to three (Tallahassee, Jacksonville, and Tifton).

Table 1 Standard deviation ratios (downscaling/observation, CFS/observation), root mean square errors [mm] and correlations for MAM (left three columns) and JJA (right three columns) precipitation for the selected local cities shown in Fig. 8

	MAM (spring)						JJA (summer)					
	std/std (O)		RMSE		Corr.		std/std (O)		RMSE		Corr.	
	D	C	D	C	D	C	D	C	D	C	D	C
Tallahassee	0.54	0.49	122	128	0.38	0.28	0.61	0.29	135	165	0.50	0.14
Jacksonville	0.51	0.65	81	173	0.63	0.25	0.69	0.39	111	137	0.42	0.09
Orlando	0.49	0.57	87	177	0.57	0.21	0.42	0.17	156	192	0.28	0.04
Miami	0.61	0.70	75	138	0.43	0.18	0.57	0.21	163	173	0.33	−0.15
Atlanta	0.41	0.55	80	247	0.48	0.09	0.63	0.65	122	333	0.32	0.07
Tifton	0.62	0.64	78	202	0.58	0.10	0.75	0.57	97	251	0.44	0.10
Birmingham	0.38	0.41	98	166	0.32	0.06	0.75	0.71	115	178	0.23	0.08
Montgomery	0.46	0.40	112	148	0.41	0.19	0.73	0.56	144	150	0.30	0.20

D and C in the third row, respectively, stand for downscaling and CFS

4.3 Skill evaluations (error variance, correlation, and categorical predictability)

Predictive skill for seasonal precipitation was evaluated and compared in further detail at individual grid points by several skill measures. Figure 10 illustrates the distribution of the relative error variances (REV) and anomaly correlations computed from the CFS and downscaled data, respectively. REV and correlation were calculated at each local grid point. The reference forecast when calculating the REV is the observed climatology. Also, seasonal climatology has been removed before calculating the correlations. The REV of the CFS data is greater than two (Fig. 10a) over most of region except for the Florida panhandle and southern Alabama. These REVs have been significantly improved by downscaling. As shown in Fig. 10b, the REV of the downscaled data lies in 0.6–1.4, with lower values over Georgia and Florida.

Anomaly correlation of the downscaled precipitation was compared with the CFS precipitation in the right panel of Fig. 10. Distributions of correlations from downscaling reveal wide variations in skill between grid points (Fig. 10d). Correlations range from 0.3 to 0.6 over most grid points over Georgia and the Florida peninsula except for the southeastern tip of Florida. Alabama and the western Florida panhandle areas exhibit relatively lower correlations than Georgia. Compared with correlations by downscaling, the CFS data tend to exhibit lower correlations (0–0.2) with observation (Fig. 10c). Increases in correlations through the application of downscaling are largest in Florida and Georgia, and moderate in Alabama (Fig. 10c, d). The present downscaling has improved the correlation over 1,156 grid points out of a total of 1,252 grid points (i.e., 92%). However, the number of grid points that satisfy the statistical significance at 90% confidence is 710 out of total of 1,252 grids (i.e., 57%). Also, 43% out of

the total area exceeds the statistical significance threshold at 95% confidence.

Compared with surface T_{max} addressed in Lim et al. (2007), the downscaled precipitation reveals relatively lower correlation with observed precipitation. Previous studies have described difficulties in obtaining demonstrable predictive skill on seasonal prediction of local precipitation (Schmidli et al. 2007), especially for summer (Murphy 1999). The Southeast US has been identified as a difficult region for prediction of summer precipitation due to the dominant local-scale convective processes.

Categorical predictability on the seasonal anomalies was assessed at individual grid points in terms of the HSS (Heidke 1926; Jolliffe and Stephenson 2003). Two kinds of classifications were considered in this study as they were described in detail in Sect. 3.3. The spatial pattern of HSS in the left panel of Fig. 11 clearly shows the positive score values over most grid points [1,199 grid points (96%)] from downscaling (Fig. 11a), indicating a skill greater than random forecast. Note that if the probability of correct forecasts is merely expected by chance in the absence of any forecasting skill, the HSS results in zero based on its formula (Heidke 1926; Barnston 1992). Many grid points have HSSs exceeding 0.1, with some reaching 0.5 over Georgia and the Florida peninsula. On the other hand, predictability by the CFS data shown in Fig. 10b reveals mostly the HSS values from −0.1 to 0.1, suggesting low predictability for seasonal precipitation. 1185 grid points (95%) show higher HSS by downscaling. Higher HSSs by downscaling are again found for three category predictability as shown in Fig. 11d, e. At 1,098 grid points (88%) three category HSS by downscaling is positive, while 581 grid points (46%) show positive HSS by CFS. At 1,003 grid points (80%), three category HSS by downscaling is higher than CFS.

Fig. 10 *Left column*
Geographical distribution of the
relative error variance based on
observed climatology for the
CFS (*upper panel*) and the
downscaled seasonal
precipitation (*lower panel*). The
scale is denoted by *color bar* on
the bottom (dimensionless).
Right column Same as the left
column but for the seasonal
anomaly correlation. Seasonal
climatology has been removed
before calculating correlations
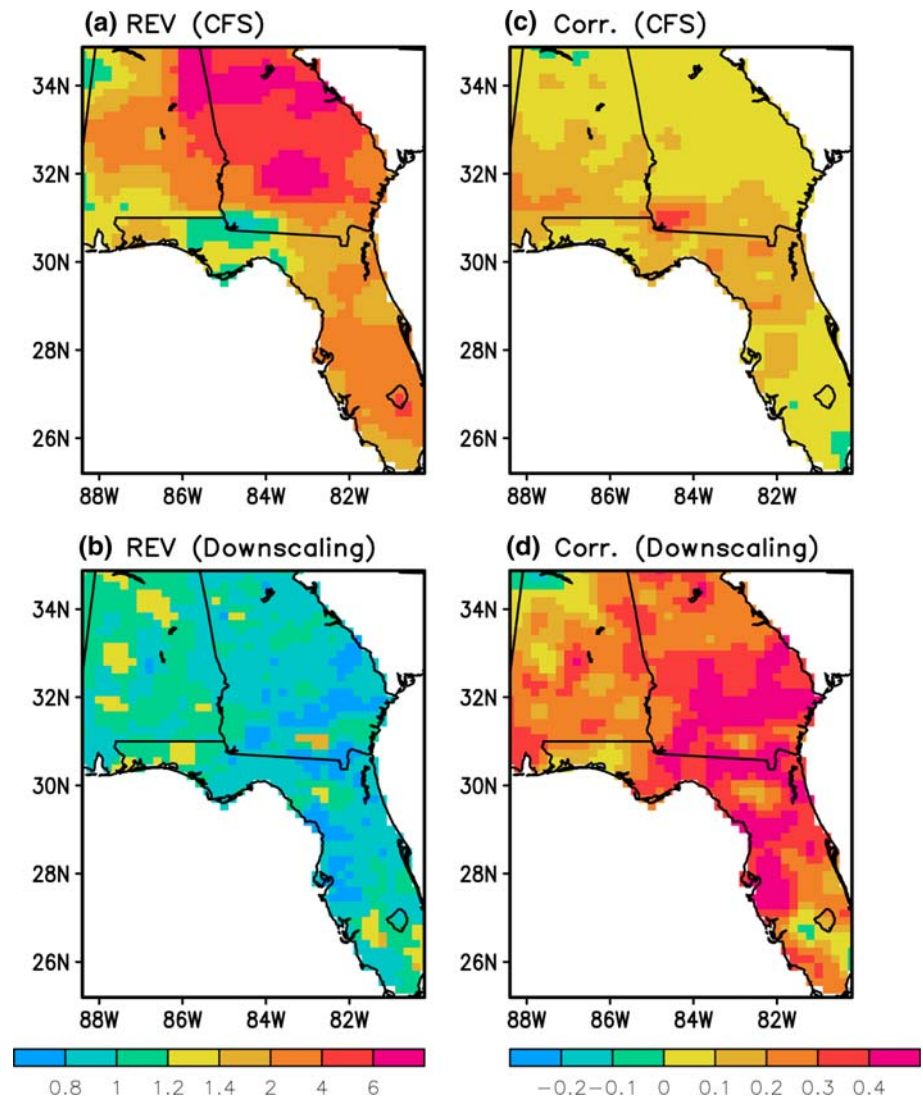
The HSS of the downscaled seasonal anomalies were additionally compared with the localized CFS into 20 km grids by OA and bias correction (Fig. 11c, f). Two-category HSS patterns reveal better prediction through downscaling (Fig. 11a, c). 988 grid points (79%) exhibit higher HSS by downscaling. As shown in Fig. 11c, a majority of HSSs from CFS range between −0.1 and 0.2 and downscaled data (Fig. 11a) exhibit generally higher HSSs than the CFS by OA and bias correction. Domain averaged HSS is 0.21 (downscaling) and 0.09 (CFS), respectively. These higher HSSs indicate that the present downscaling better explains the local-scale seasonal anomaly, which cannot be adequately reproduced by bias corrected OA. Three category HSSs (Fig. 11d, f) represent similar features. However, the domain averaged HSS is reduced to, respectively, 0.11 (downscaling) (Fig. 11d) and 0.03 (CFS) (Fig. 11f). The number of grid points showing greater HSS by downscaling has also reduced to 928 (74%).

4.4 Daily and subseasonal precipitation statistics (heavy rainfall days and dry spells)

There have been increases in the annual frequency of heavy rainfall days over the past several decades in the US (Higgins et al. 2007). Such heavy rainfall events, and dry spells, play a significant role in determining the agricultural yields and regional hydrology. Accurate prediction of the frequency of these events is, therefore, essential for successful agricultural production and water management over the southeast US (Robertson et al. 2007). We now investigate the frequency (MAMJJA) of heavy rainfall days and subseasonal dry spells produced by the downscaling and the localized CFS by OA and bias correction. How we define and count the heavy rainfall days each year was described in detail in Sect. 3.4.

Figure 12 depicts the interannual change in the number of heavy rainfall days for the representative locations. In

Fig. 11 Geographical distribution of categorical predictability in terms of HSS for the downscaled seasonal precipitation and the CFS. Two categories (above/below seasonal climatological average), and three categories (above/near/below seasonal climatological average) are considered for this HSS calculation. *The left column, from the top row*, represents the two-category HSS calculated from downscaling, the CFS, and objectively analyzed CFS with bias correction. The right column is the same as the left column but for three category HSS distribution
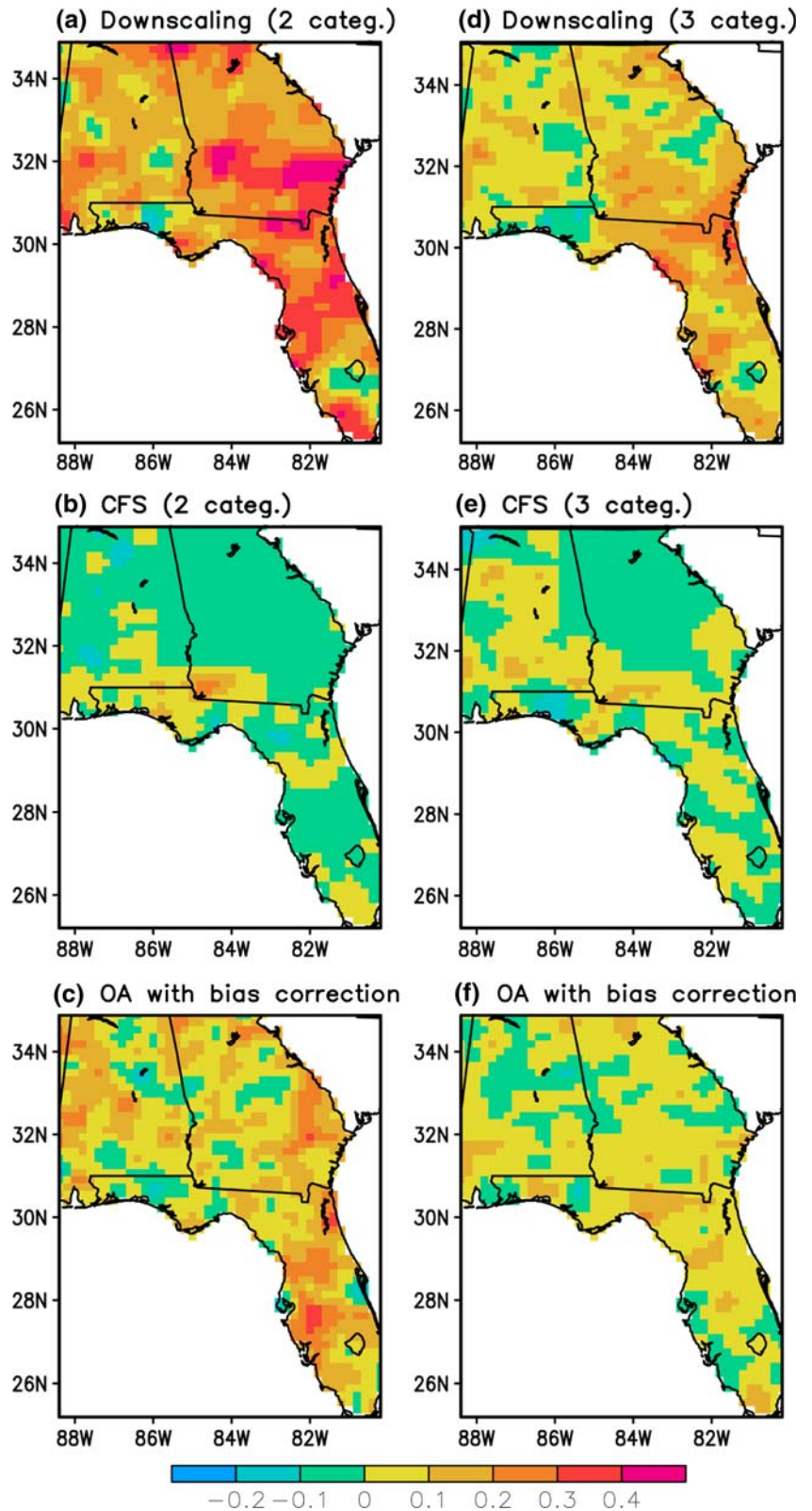
this figure, the threshold value that defines the heavy rainfall is 1 standard deviation above climatology (Saha et al. 2006). In other words, if there is a rainy day when the amount is larger than the sum of the daily climatological mean and 1 standard deviation, it is considered to be a heavy rainfall day. Blue bars (localized CFS by OA and
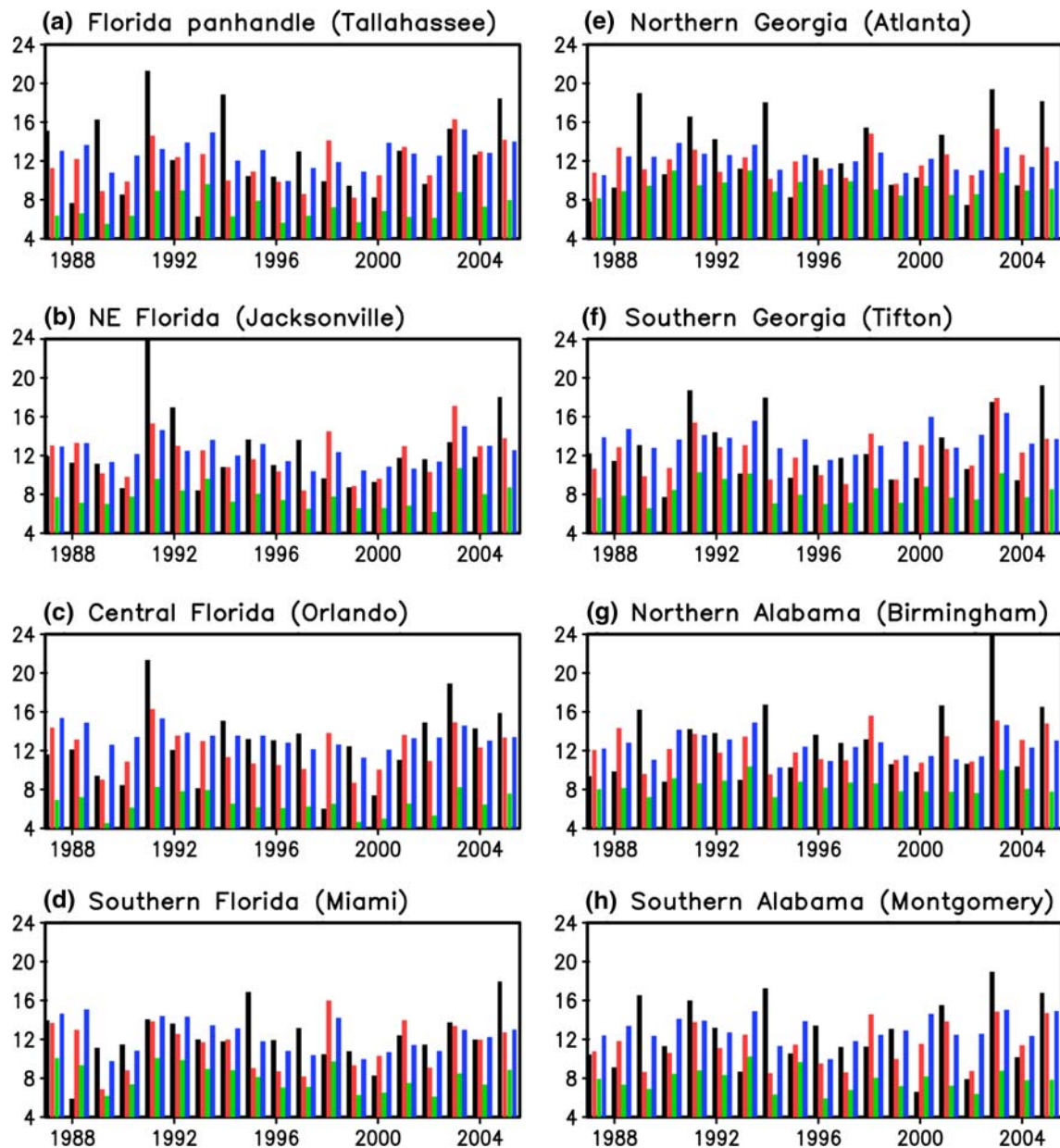
Fig. 12 Year-to-year variation of the annual frequency of heavy rainfall days. Heavy rainfall event is defined as a day when the rainfall amount is greater than one standard deviation above the observed daily climatology. *Black, red, green, and blue bars*, respectively, represent the frequency variation in time by observation, downscaling, localized CFS by OA only, and localized CFS by OA bias-correction) indicate that the bias correction proposed in this study corrects the underestimation problem that can arise when only OA is applied (green bars). Obviously, OA will be limited in terms of properly capturing the short-term extreme events due to the inherent interpolation process. However, the CFS with OA and bias correction still has a limited ability to properly reproduce the observed number of annual heavy rainfall days. For example, it (blue bar) exhibits less distinct interannual change in amplitude and bias correction. Ratio of the standard deviation to the observational standard deviation (S), root mean square error (R), and correlation (C) with the observation are provided in the upper corner of each panel. D and C in parentheses stand for downscaling and CFS, respectively

than the downscaled series (red bar) (see standard deviation ratio in each panel). This little amplitude change is much clearer over Orlando and Atlanta, indicating the need for downscaling for a more desirable capture of observed extreme events. Downscaling shows relatively larger interannual changes in amplitude than the CFS with OA and bias correction (compare the standard deviation ratios). Also, observed variation is particularly well reproduced by the downscaling since 1999. Correlation comparisons

noted in each panel clarify that the present downscaling outperforms the localized CFS by OA and bias correction. It is not encouraging, however, that only four cities (Jacksonville, Orlando, Atlanta, and Tifton) satisfy the statistical significance at 90% confidence in terms of correlation. As addressed in Gershunov et al. (2003) and Saha et al. (2006), successful prediction of rainfall extremes for the growing season across the southeast US remains challenging.

We now assess the categorical predictability on the frequency of heavy rainfall day each year in terms of HSS. Two different threshold values defining the heavy rainfall (i.e., 0.5 std. + climatological daily precipitation, and 1 std. + climatological daily precipitation) were considered.

Fig. 13 Geographical distribution of categorical predictability in terms of HSS for the frequency of daily heavy rainfall events each year. Threshold value for heavy rainfall is the daily rainfall amount greater than half a standard deviation above observed daily climatology. The *left column, from the top row*, represents the two-category HSS calculated from downscaling, localized CFS by OA and bias correction, and their difference (downscaling minus localized CFS by OA and bias correction). The right column is the same as the left column but for three category HSS distribution
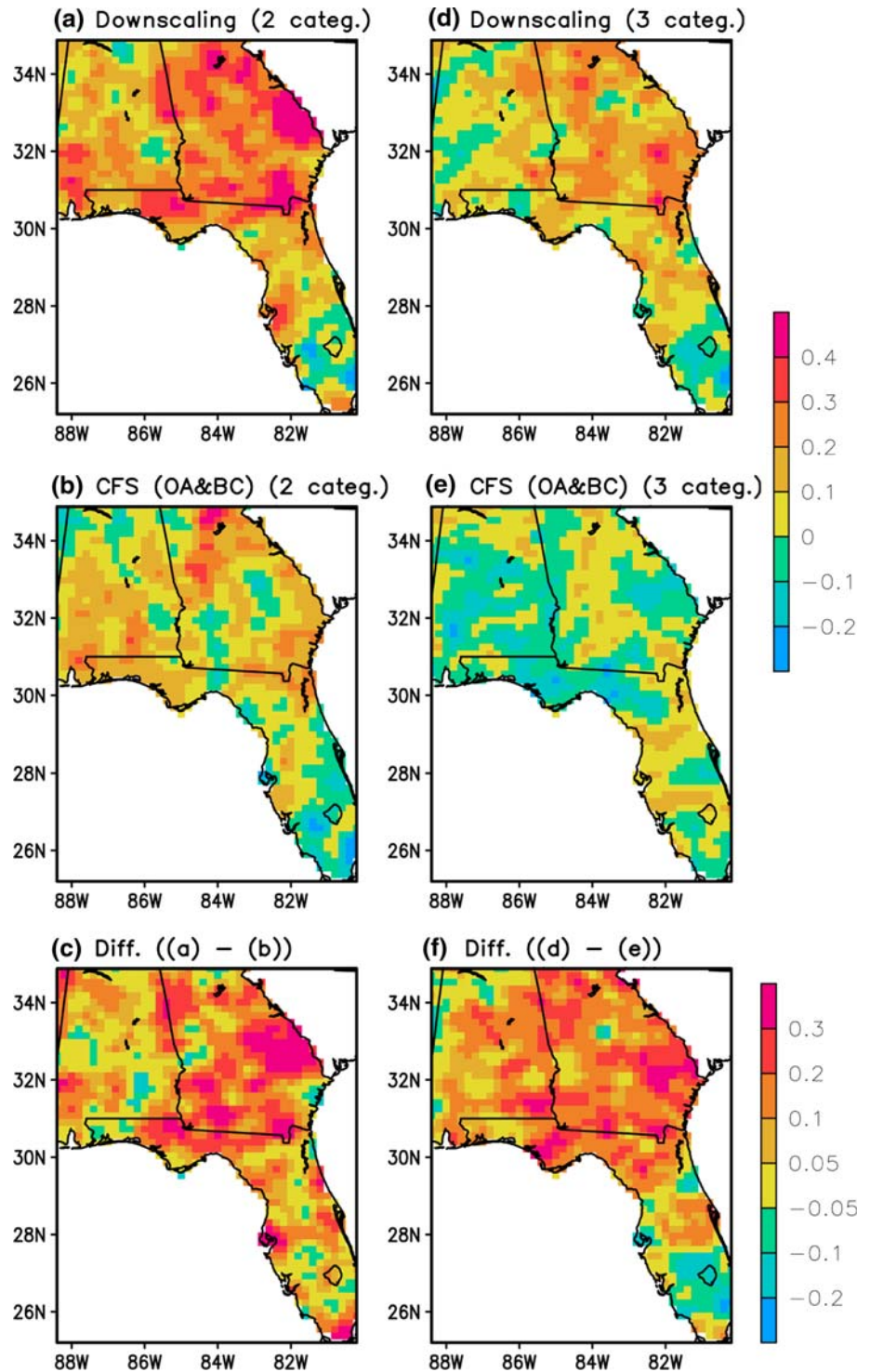
Then we counted the number of heavy rainfall days each year and calculated the HSS. Two-category (above/below average) and three category statistics (above/near/below average) are, respectively, considered for HSS calculation. The HSSs calculated from the downscaled data were compared with those from the localized CFS by OA and bias correction. Figure 13 (0.5 std.) and 14 (1 std.) depict the resulting HSSs at each local grid point. The distribution of HSSs in Fig. 13a reveals the reliable prediction of the number of heavy rainfall days each year by downscaling. HSS values are positive but for a few grid points scattered over northern Alabama and southern Florida. Most areas, including Georgia, Alabama, and central and northern Florida, exhibit HSSs exceeding 0.1 and approaching up to 0.5. The result from the CFS also shows the positive HSSs over grid points (0–0.2) but concurrently, negative HSSs are observed over many grid points (Fig. 13b). A comparison indicates that HSS values by downscaling are, in general, greater than those of the CFS, as is clarified in the difference map in Fig. 13c. 1,035 grid points (83%) show higher HSS by downscaling. All area averaged HSS is, respectively, 0.20 (downscaling) and 0.07 (CFS). The similar relative difference between downscaling and localized CFS is found again from the three category HSS evaluation on the right column of Fig. 13. Nearly all grid points except for southern Florida and northwestern Alabama [1,049 (84%)] show improved HSS by downscaling (Fig. 13f). However, HSS values are, overall, smaller than those for two-category predictability. Georgia, northeastern Florida, and eastern Alabama show HSSs at least higher than 0.1, while remaining areas show lower HSSs (Fig. 13d). HSSs by the CFS are negative in a majority of grid points (Fig. 13e). Figure 14 shows a quite similar distribution of HSSs. The area averaged HSS for two category classification is, for example, 0.21 (downscaling) (Fig. 14a) and 0.06 (CFS) (Fig. 14b). The same calculation for the three category HSS yields, respectively, 0.13 (downscaling) (Fig. 14d) and −0.01 (CFS) (Fig. 14e). Reasonable probabilistic prediction of heavy rainfall frequency is valuable in that annual rainfall has a strong contribution from extreme events (Higgins et al. 2007). Differences among data produced by downscaling, localized CFS by OA and bias correction, and OA only, respectively, are good indicators that the reasonable downscaling is indeed essential for better prediction of extreme events at fine spatial scales, although the pronounced improvement is unfortunately not achieved for frequency of dry spells in the following discussion.

The same calculation of HSS for the annual frequency of dry spells (accumulated precipitation of less than 0.1 mm/day for a week) (Robertson et al. 2004) shows a lower skill than that for seasonal precipitation anomalies and annual heavy rainfall days. As shown in Fig. 15a, scores greater than ∼0.2 by downscaling are limited over southern Alabama and northern and eastern Georgia. Nearly zero values or negative HSS values are seen over many other regions. Comparison between the downscaling (Fig. 15a) and the localized CFS by OA and bias correction (Fig. 15b) indicates the substantial increase in HSSs by downscaling over Alabama and Georgia (Fig. 15c). However, all area averaged HSS by the downscaling remains 0.10 (CFS 0.03), which is lower than that for the seasonal precipitation and annual heavy rainfall days. The identified features here are seen again for three category HSSs and different definitions of the dry spell [e.g., a 10 day rainless period (Robertson et al. 2004; Higgins et al. 2008)]. Area averaged HSS for definition of 10 day rainless period is, respectively, 0.10 (downscaling) and 0.06 (bias corrected OA) (Figure not shown).

The distribution of HSSs demonstrates that the downscaling reasonably contributes to the local-scale prediction of heavy rainfall frequency. However, results also hint at the difficulty of local-scale prediction of growing season precipitation. Prevailing rainfall events over this region are convective in nature, indicating that most rainfall, particularly for the summer season, is not directly associated with the large-scale atmospheric circulation. This provides poor conditions for accurate downscaling from the large-scale fields (Trigo and Palutikof 2001; Friederichs and Hense 2007). Specifically, prediction of subseasonal dry spells should be significantly improved in order to increase the demonstrable skill in further studies.

5 Concluding remarks and discussion

Coarsely resolved daily precipitation simulated from the NCEP/CFS (2.5° resolution) has been downscaled to a fine spatial scale of 20 km × 20 km for the southeastern US, covering Florida, Georgia, and Alabama, by the CSEOF-based statistical downscaling model introduced in Sects. 1 and 3. The main purpose of this study is to better predict the seasonal precipitation and extreme event frequencies at a finer spatial resolution than the coarse-scale model. Previous studies using the coarsely resolved model data have discussed difficulties in downscaling precipitation for summer (Murphy 1999; Friederichs and Hense 2007) with greater success for winter (Cocke et al. 2007). Strong interannual variation of precipitation, resulting from strong dry spells, and frequent heavy convective rainfalls, accompanied by either local thunderstorms or hurricanes, represent additional prediction challenges over the southeastern US. In this study, 19-year CFS precipitation seasonally integrated for the crop growing season (e.g., MAMJJA) with ten members has been downscaled for the period of 1987 to 2005. For skill assessment, the

Fig. 14 Same as Fig. 13 but for the threshold value of 1 standard deviation above observed daily climatology
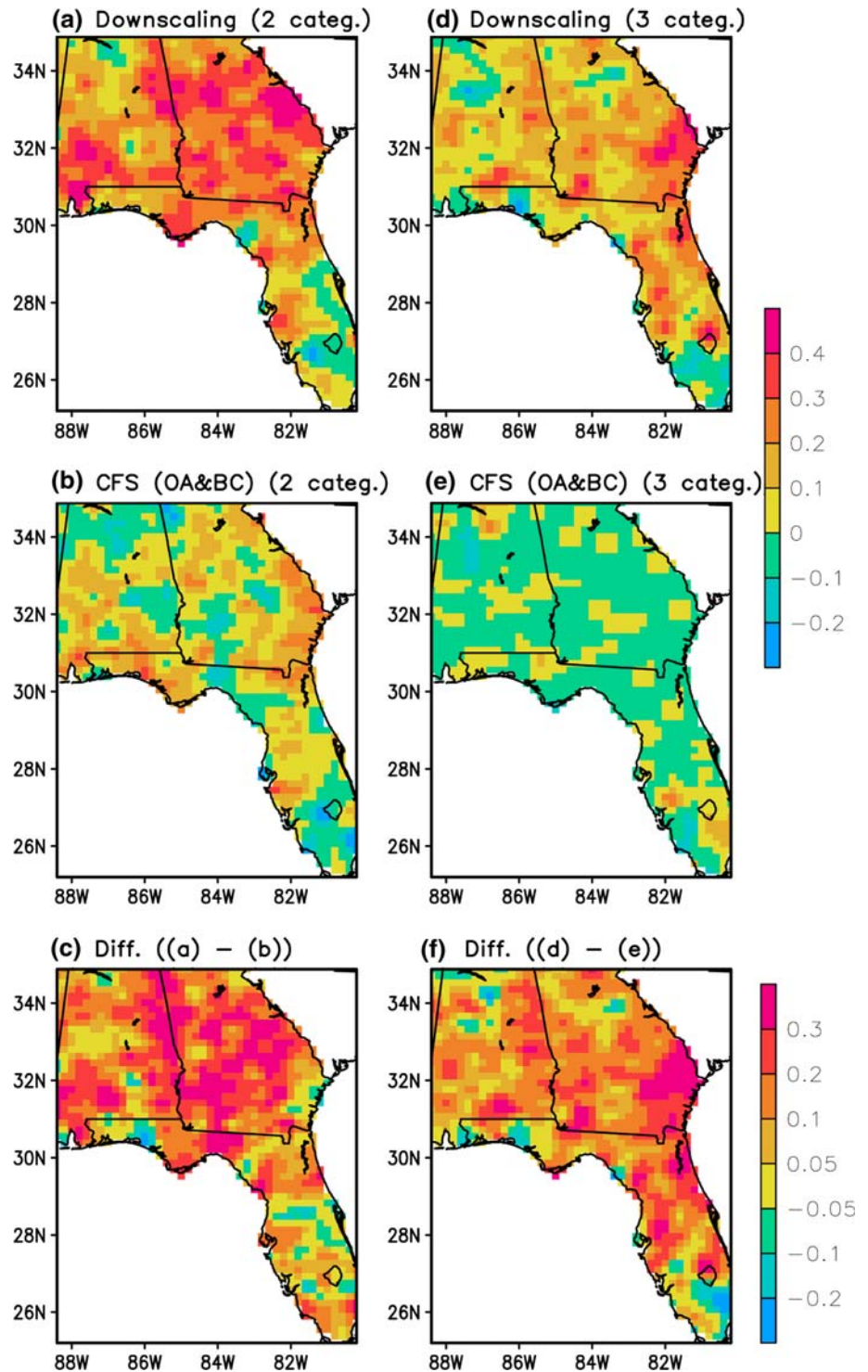

downscaled precipitation was compared with the localized CFS at 20 km resolution. Forecast error has been also investigated by comparing downscaled forecasts with reference estimates.

The results demonstrate that the downscaling proposed in this study outperforms the coarse-scale CFS and the localized CFS derived from OA and bias correction in

terms of the seasonal prediction of precipitation and heavy rainfall frequencies. The downscaled seasonal precipitation patterns and their long-term temporal variation better reproduce the observed precipitation than the CFS. The ratio of the standard deviations, RMSE, and correlation has been improved by downscaling. Error statistics compared with those of reference estimates (e.g., observed

Fig. 15 Same as Fig. 13 but for the subseasonal dry spell. Dry spell is defined as a week period with the accumulated rainfall amount less than 0.1 mm/day
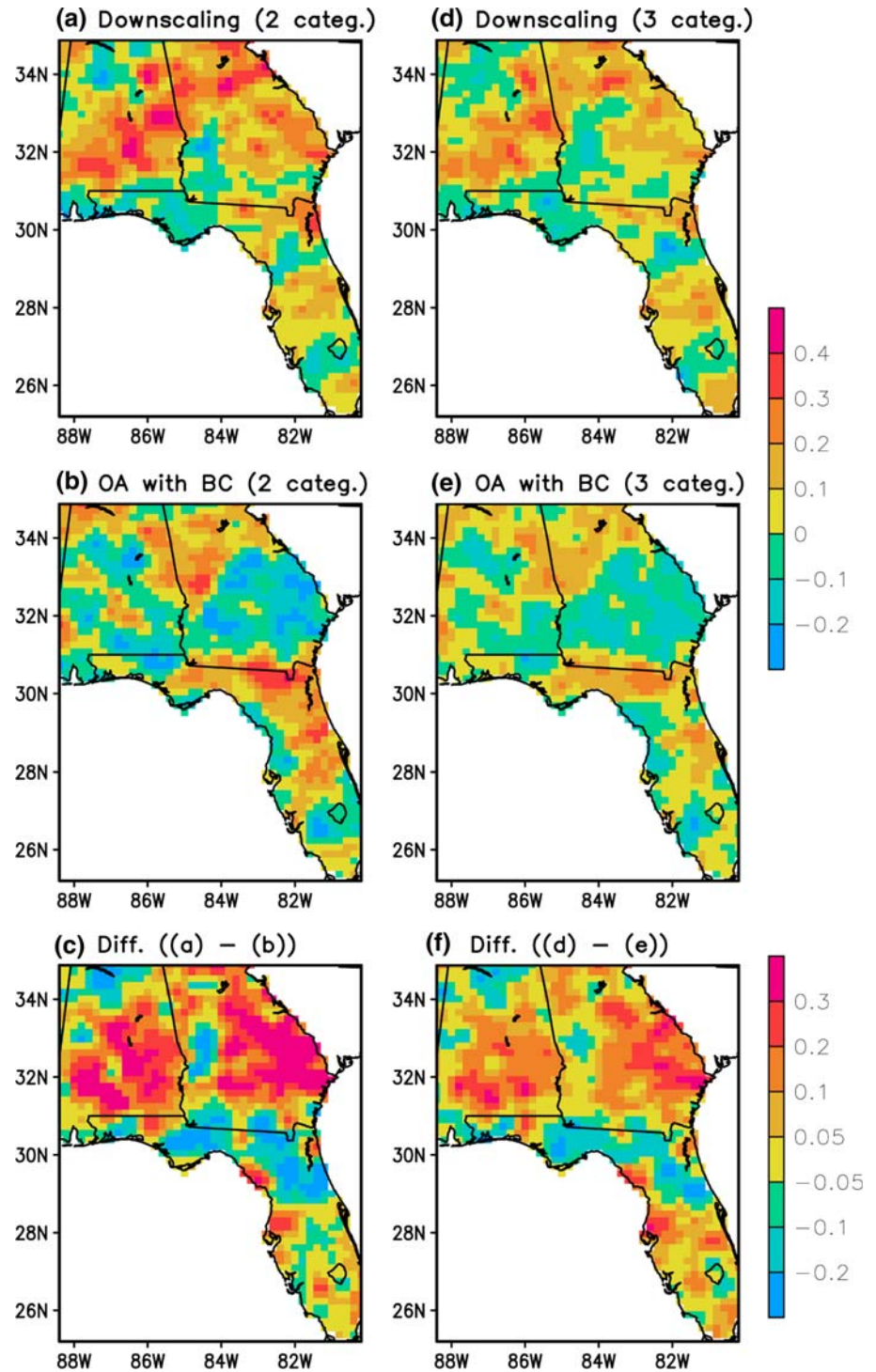
climatology) and wet biases found in the CFS have been substantially reduced by the downscaling. For instance, the relative error variance of the downscaled data to the reference error variance (e.g., observed climatology) lies in the 0.6–1.4 range, while the CFS yields a relative error variance larger than two over a majority of grid points. Downscaled seasonal anomalies exhibit correlations from 0.3 up to 0.6, in general, over the Florida peninsula and central and southern Georgia. This correlation range corresponds to the correlation increase by 0.1–0.5 from the unskillful CFS. For inland regions such as northern Georgia and Alabama, however, correlations for downscaled anomalies are apparently not high. Causes of the relatively lower correlation over inland regions and higher

correlation over Florida and southern Georgia need to be further investigated. It appears that the downscaled seasonal predictive skill is, to a certain extent, dependent on the coarse-scale model capability. This indicates that the successful global model performance would be preferred to obtain more desirable downscaled fields. Because of the poor skill of the large-scale CFS, the increased correlations found over nearly all grid points (92% of the total number of grid points) by downscaling are not statistically significant at all grid points. Approximately 60% out of the total number of grid points satisfy the statistical significance at 90% confidence.

Categorical prediction is also improved through application of downscaling. Considering two-category predictability (above/below average), the localized CFS by OA and bias correction exhibit HSSs ranging from −0.1 to 0.2 over a majority of grid points. HSSs computed from downscaled data range from 0.1 to 0.5, with the exception of a few grid points. The downscaled data also exhibit better performance for frequency of heavy rainfall days. Area averaged HSSs by downscaling are 0.20–0.21 for different definitions of a heavy rainfall day, while the HSSs by CFS result in 0.06–0.07. Specifically, the interannual amplitude change of the frequency is much less pronounced by CFS than by downscaling.

Our study has shown the potential improvement of local scale predictive skill achieved through downscaling of coarse resolution CFS output. However, the improved skill values were not statistically significant all over the grid points. In addition, skill was not yet very encouraging for the prediction of subseasonal dry spell frequency. A variety of downscaling attempts under different downscaling strategies and configurations will be continued in the next study for further improvement of predictive skill.

References

Baigorria GA, Hansen JW, Ward N, Jones JW, O'Brien JJ (2008) Assessing predictability of cotton yields in the southeastern United States based on regional atmospheric circulation and surface temperatures. J Appl Meteor Climatol 47:76–91

Barnston AG (1992) Correspondence among the correlation, RMSE, and Heidke forecast verification measures; Refinement of the Heidke score. Weather Forecast 7:699–709

Cocke S, La Row TE, Shin DW (2007) Seasonal rainfall prediction over the southeast U.S. using the FSU nested regional spectral model. J Geophys Res 112:D04106. doi:10.1029/2006JD007535

Coulibaly P, Dibike YB, Anctil F (2005) Downscaling precipitation and temperature with temporal neural networks. J Hydrometeorology 6:483–496

Cressman GP (1959) An operational objective analysis system. Mon Weather Rev 87:367–374

Duffy PB, Arritt RW, Conquard J, Gutowski W, Han J, Iorio J, Kim J, Leung L-R, Roads J, Zeledon E (2006) Simulations of present and future climates in the western United States with four nested regional climate models. J Clim 19:873–895

Feddersen H, Andersen U (2005) A method for statistical downscaling of seasonal ensemble predictions. Tellus 57A:398–408

Fennessy MJ, Shukla J (2000) Seasonal prediction over North America with a regional model nested in a global model. J Clim 13:2605–2627

Friederichs P, Hense A (2007) Statistical downscaling of extreme precipitation events using censored quantile regression. Mon Weather Rev 135:2365–2378

Fuentes U, Heimann D (2000) An improved statistical-dynamical downscaling scheme and its application to the Alpine precipitation climatology. Theor Appl Climatol 65:119–135

Gershunov A, Barnett T, Cayan D (2003) Heavy daily precipitation frequency over the contiguous United States: sources of climate variability and seasonal predictability. J Clim 16:2752–2765

Giorgi F (1990) Simulation of regional climate using a limited area model nested in a general-circulation model. J Clim 3:941–963

Groisman PY, Legates DR (1994) The accuracy of United States precipitation data. Bull Amer Meteor Soc 75:215–227

Heidke P (1926) Berechnung des Erfolges und der Gute der Windstarkevorhersagen im Sturmwarnungsdienst. Geografts Ann 8:301–349

Hewitson BC, Crane RG (1996) Climate downscaling: techniques and application. Clim Res 7:85–95

Higgins RW, Silva V, Larson J, Shi W (2007) Relationship between climate variability and fluctuations in daily precipitation over the United States. J Clim 15:3561–3579

Higgins RW, Silva VBS, Kousky VE, Shi W (2008) Comparison of daily precipitation statistics for the United States in observations and in the NCEP Climate Forecast System. J Clim. doi:10.1175/2008JCLI2339.1

Hong SY, Leetma A (1999) An evaluation of the NCEP RSM for regional climate modeling. J Clim 12:592–609

Hu Q, Feng S (2001) Variations of teleconnection of ENSO and interannual variation in summer rainfall in the central United States. J Clim 14:2469–2480

Huth R (2002) Statistical downscaling of daily temperature in central Europe. J Clim 15:1731–1742

Huth R, Kysely J (2000) Constructing site-specific climate change scenarios on a monthly scale using statistical downscaling. Theor Appl Climatol 66:13–27

Ji Y, Vernekar AD (1997) Simulation of the Asian summer monsoons of 1987 and 1988 with a regional model nested in a global GCM. J Clim 10:1965–1979

Jolliffe IT, Stephenson DB (2003) Forecast verification: a practitioner's guide in atmospheric science. Wiley, Hoboken, p 240

Kanamitsu M, Ebisuzaki W, Woollen J, Yang SK, Hnilo JJ, Fiorino M, Potter GL (2002) NCEP-DOE AMIP-II Reanalysis (R-2). Bull Amer Meteor Soc 83:1631–1643

Kim JE, Hong SY (2007) Impact of soil moisture anomalies on summer rainfall over East Asia: a regional climate model study. J Clim 20:5732–5743

Kim KY, North GR (1997) EOFs of harmonizable cyclostationary processes. J Atmos Sci 54:2416–2427

Kim KY, Wu Q (1999) A comparison study of EOF techniques: analysis of nonstationary data with periodic statistics. J Clim 12:185–199

Kim J, Miller NL, Farrara JD, Hong SY (2000) A seasonal precipitation and stream flow hindcast and prediction study in the western United States during the 1997/98 winter season using a dynamic downscaling system. J Hydrometeorology 1:311–329

Leung LR, Qian Y, Bian X (2003) Hydroclimate of the western United States based on observations and regional climate simulation of 1981–2000. Part I: seasonal statistics. J Clim 16:1892–1911

Liang XZ, Pan J, Zhu J, Kunkel KE, Wang JXL, Dai A (2006) Regional climate model downscaling of the U.S. summer climate and future change. J Geophys Res 111:D10108. doi:10.1029/2005JD006685

Lim YK, Kim KY (2006) A new perspective on the climate prediction of Asian summer monsoon precipitation. J Clim 19:4840–4853

Lim YK, Shin DW, Cocke S, La Row TE, Schoof JT, O'Brien JJ, Chassignet EP (2007) Dynamically and statistically downscaled seasonal simulation of maximum surface air temperature over the southeastern United States. J Geophys Res 112:D24102. doi:10.1029/2007JD008764

Mahrt L, Pan HL (1984) A two-layer model of soil hydrology. Bound-Layer Meteorol 29:1–20

Misra V, Dirmeyer PA, Kirtman BP (2003) Dynamical downscaling of seasonal simulations over South America. J Clim 16:103–117

Murphy J (1999) An evaluation of statistical and dynamical techniques for downscaling local climate. J Clim 12:2256–2284

Pandey GR, Cayan DR, Dettinger MD, Georgakakos KP (2000) A hybrid orographic plus statistical model for downscaling daily precipitation in northern California. J Hydrometeorology 1:491–506

Ramírez MCV, Ferreira NJ, Velho HFC (2006) Linear and nonlinear statistical downscaling for rainfall forecasting over southeast Brazil. Weather Forecast 21:969–989

Reusch DB, Alley RB (2002) Automatic weather stations and artificial neural networks: improving the instrumental record in west Antarctica. Mon Weather Rev 130:3037–3053

Robertson AW, Kirshner S, Smyth P (2004) Downscaling of daily rainfall occurrence over northeast Brazil using a hidden Markov model. J Clim 17:4407–4424

Robertson AW, Ines AVM, Hansen JW (2007) Downscaling of seasonal precipitation for crop simulation. J Appl Meteor Climatol 46:677–693

Saha S, Nadiga S, Thiaw C, Wang J, Wang W, Zhang Q, Van den Dool HM, Pan HL, Moorthi S, Behringer D, Stokes D, Peña M, Lord S, White G, Ebisuzaki W, Peng P, Xie P (2006) The NCEP climate forecast system. J Clim 19:3483–3517

Salathé EP (2005) Downscaling simulations of future global climate with application to hydrologic modeling. Int J Climatol 25:419–436

Schmidli J, Goodess CM, Frei C, Haylock MR, Hundecha Y, Ribalaygua J, Schmith T (2007) Statistical and dynamical downscaling of precipitation: an evaluation and comparison of scenarios for the European Alps. J Geophys Res 112:D04105. doi:10.1029/2005JD007026

Schoof JT, Pryor SC (2001) Downscaling temperature and precipitation: a comparison of regression-based methods and artificial neural networks. Int J Climatol 21:773–790

Schoof JT, Shin DW, Cocke S, LaRow TE, Lim YK, O'Brien JJ (2009) Dynamically and statistically downscaled seasonal temperature and precipitation hindcast ensembles for the southeastern USA. Int J Climatol. doi:10.1002/joc.1717

Sun L, Moncunill DF, Li H, Moura AD, Filho FDADS, Zebiak SE (2006) An operational dynamical downscaling prediction system for nordeste Brazil and the 2002–04 real-time forecast evaluation. J Clim 19:1990–2007

Trigo RM, Palutikof JP (2001) Precipitation scenarios over Iberia: a comparison between direct GCM output and different downscaling techniques. J Clim 14:4422–4446

von Storch H, Zorita E, Cubasch U (1993) Downscaling of global climate change estimates to regional scales: an application to Iberian rainfall in wintertime. J Clim 6:1161–1171

Widmann M, Bretherton CS, Salathe EP Jr (2003) Statistical precipitation downscaling over the northwestern United States using numerically simulated precipitation as a predictor. J Clim 16:799–816

Wilby RL, Wigley TML (1997) Downscaling general circulation model output: a review of methods and limitations. Prog Phys Geogr 21:530–548

Wilby RL, Wigley TML, Conway D, Jones PD, Hewitson BC, Main J, Wilks DS (1998) Statistical downscaling of general circulation model output: a comparison of methods. Water Resour Res 34:2995–3008

Wilks DS (1999) Multisite downscaling of daily precipitation with a stochastic weather generator. Clim Res 11:125–136

Wood AW, Maurer EP, Kumar A, Lettenmaier DP (2002) Long-range experimental hydrologic forecasting for the eastern United States. J Geophys Res 107(D20):4429. doi:10.1029/2001JD000659

Wood AW, Kumar A, Lettenmaier DP (2005) A restrospective assessment of National Center for Environmental Prediction climate model-based ensemble hydrologic forecasting in the western United States. J Geophys Res 110:D04105. doi:10.1029/2004JD004508